PERGAMON

Journal of Structural Geology 23 (2001) 1631–1652

JOURNAL OF STRUCTURAL GEOLOGY

www.elsevier.com/locate/jstrugeo

Flexural-slip folding in the Meguma Group, Nova Scotia, Canada

Richard Horne[a,*], Nicholas Culshaw[b]

[a]*Nova Scotia Department of Natural Resources, P.O. Box 698, Halifax, Nova Scotia, Canada, B3J 2T9*
[b]*Department of Earth Sciences, Dalhousie University, Halifax, Nova Scotia, Canada, B3H 3J5*

Received 3 November 1999; accepted 19 September 2000

Abstract

Flexural-slip folding has been established for two anticlines in the Meguma Group, Nova Scotia. Flexural slip postdates the main Acadian episode of flexural-flow fold growth and represents a late, brittle-ductile reactivation of the fold belt. Flexural-slip structures are dominated by bedding-parallel movement horizons, but include a linked system of frontal and lateral ramps and conjugate movement horizons. Slip amount calculated from displacement of discordant quartz veins, combined with vein spacing, indicates an average local shear strain of approximately 0.5. However, because flexural-slip occurred when the fold limbs were steep, the shear strain accounts for a small change in limb dip (4–8°). Variation of slip amount with spacing of movement horizons suggests progressive flexural slip was accommodated by continuous initiation of new movement horizons as well as continuing slip on existing movement horizons.

The presence of quartz veins along flexural-slip structures together with evidence for ductile deformation coeval with flexural slip suggests that slip episodes were fluid assisted and intermittent, separated by periods of ductile deformation and build up of fluid pressure. Flexural-slip veins in the Ovens Anticline are auriferous and a flexural slip model may be appropriate for other similar Meguma gold deposits.

Thrust sheets, up to 10 m thick, occurring on a fold limb are interpreted to have originated in flat box fold hinges and to have been placed onto the steep limbs of the chevron folds during the flexural slip episode. Thrusting may have assisted the transformation of a box fold into a chevron.

Keywords: Flexural slip; Anticlines; Fold belt

1. Introduction

Folding of highly anisotropic sedimentary sequences, such as metaturbidites, typically results in the development of chevron and box folds (e.g. Biot, 1965; Cobbold et al., 1971; Ramsay, 1974; Fowler and Winsor, 1996). Such folds initiate and amplify with little layer-parallel shorting (Ramsay and Huber, 1987). Development of chevron folds by flexural folding is well understood from theoretical and experimental work (de Sitter, 1958; Ramsay, 1974; Dubey and Cobbold, 1977; Behzadi and Dubey, 1980; Hudleston et al., 1996) that suggests they evolve through a variety of shape changes during progressive shortening, including modification of flat-topped box folds (Fowler and Winsor, 1996). In these studies, flexural folding is treated as a plane strain deformation with bedding-parallel shear on fold limbs directed perpendicular to the hinge. Shear from flexural folding can be accommodated homogeneously throughout the sequence (flexural flow) or localized along discrete movement horizons (flexural slip) (e.g. Ramsay and Huber, 1987).

Studies of natural folds have documented evidence of flexural slip, notably bedding-parallel movement horizons characterized by striations, slickenfibers and offset markers (e.g. Chapple and Spang, 1974; Ramsay and Huber, 1987; Tanner, 1989; Markley and Wojtal, 1996; Fowler and Winsor, 1997). There is, however, a lack of studies that quantify the amount and timing of flexural slip, largely because of the difficulty of recognizing movement horizons and determining the amount of slip which has occurred (Tanner, 1989).

Quartz veins, including bedding-parallel, saddle reef and discordant veins are commonly associated with chevron folds, and fluid pressure may play a key role in fold genesis; Price and Cosgrove (1990) and Cosgrove (1993) suggest that bedding-parallel veins provide evidence of high fluid pressure required for the development of large-scale flexural-slip folds. However, the origin of bedding-parallel veins has caused considerable debate. The principal issue is whether the veins were formed during or before the folding process (see Fowler (1996) for review).

In this paper, we present the results of a detailed investigation of flexural slip in the hinge zones of two anticlines (Lawrencetown and Ovens anticlines) within the

* Corresponding author.
E-mail address: rjhorne@gov.ns.ca (R. Horne).

0191-8141/01/$ - see front matter
PII: S0191-8141(01)00017-7

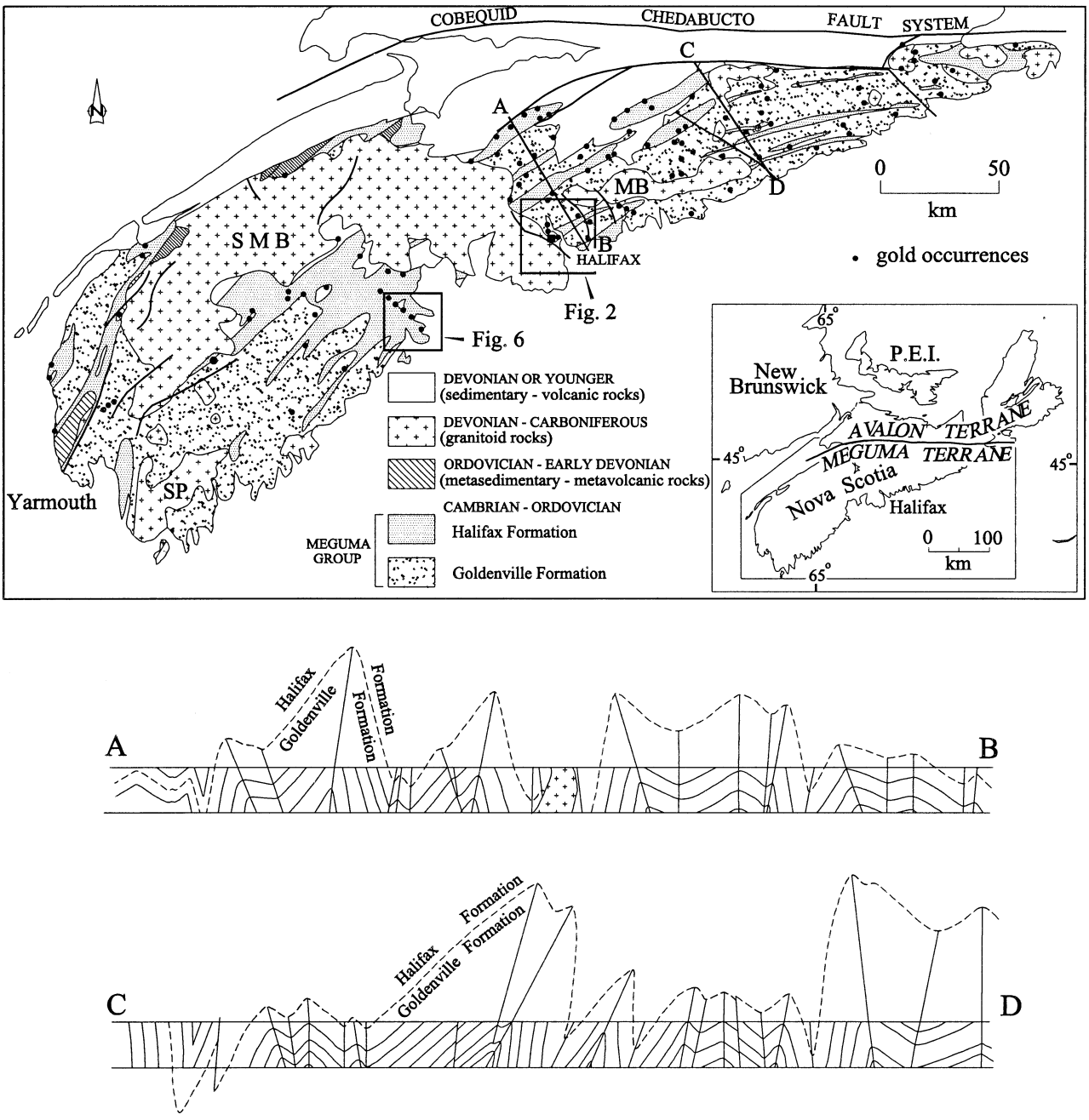

Fig. 1. Simplified geological map and cross-sections of the Meguma Terrane (after Keppie (1979)) showing the location of the Halifax and Ovens study areas and the distribution of gold deposits. Cross-sections after Fletcher and Faribault (1911). SMB = South Mountain Batholith. MB = Musquodoboit Batholith.

metasediments of the Paleozoic Meguma Group, Nova Scotia. The folds demonstrate abundant evidence of flexural slip, including features similar to those described by Tanner (1989, 1992) and also previously undescribed structures. Most importantly, the occurrence of discordant quartz veins displaced by flexural slip allows a quantitative evaluation of slip. Quartz slickenfibers and local concentrations of auriferous quartz veins occur along structures related to flexural slip and fluid pressure may have been important to flexural-slip activity. Fabric relations in large thrust sheets within the folds suggest that thrusting, which occurred during the flexural-slip event, locally aided modification of flat-topped box folds to chevrons.

2. Regional setting

The Meguma Terrane is the most outboard terrane of the Appalachians and is separated from the Avalon Terrane by the transcurrent Cobequid–Chedabucto Fault System (Fig. 1). The Meguma Terrane is dominated by Lower Paleozoic metamorphic rocks, including the Cambrian–Ordovician

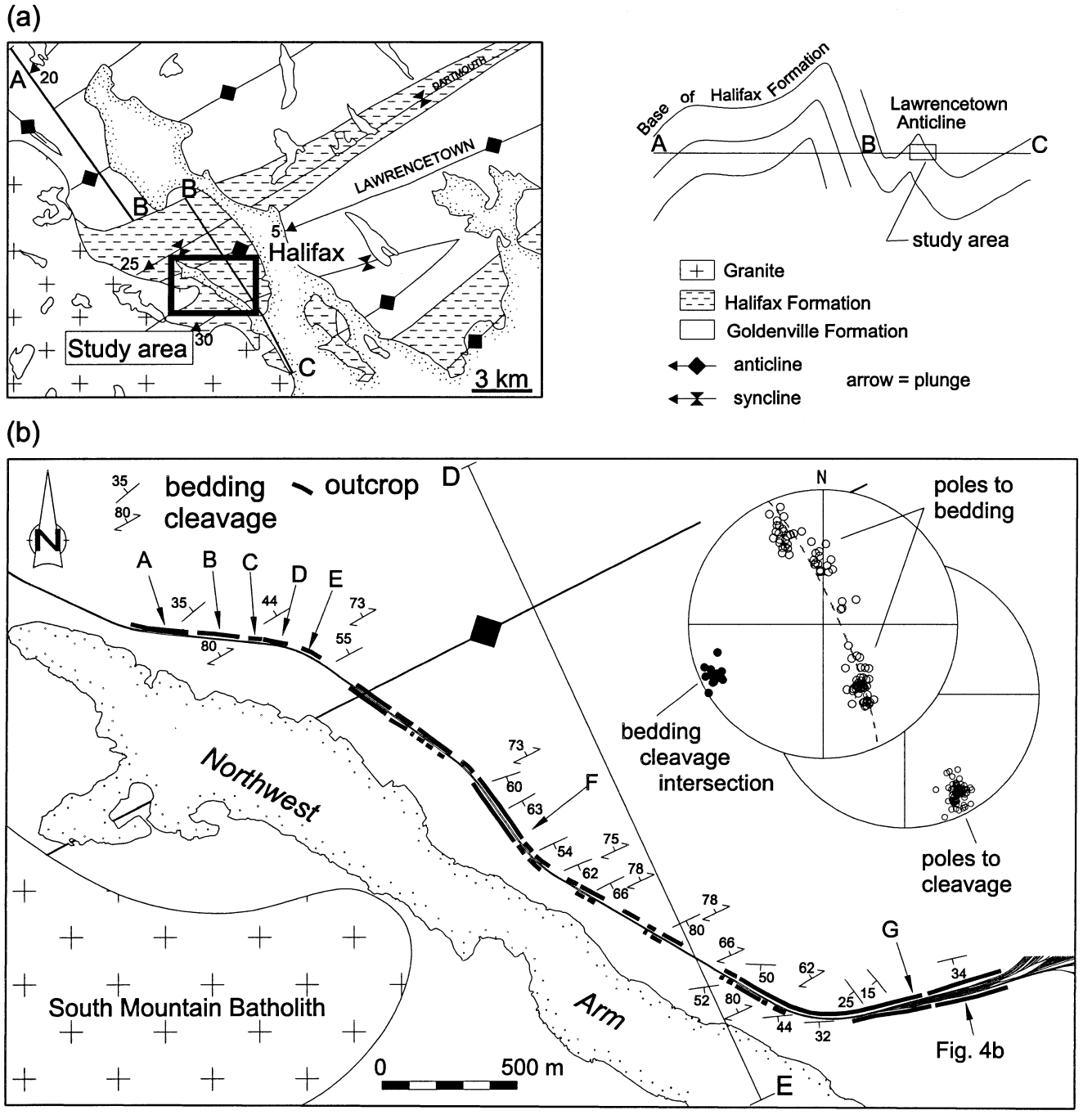

Fig. 2. (a) Geological map and cross-section of the Halifax area showing the location of the study area within the hinge of the Lawrencetown Anticline (modified from Faribault (1908)). (b) Detailed map and stereonets of structural geology of the studied section along the railway tracks. Letters (A–G) indicate location of measured sections in Fig. 3.

Meguma Group and conformably to disconfomably overlying Ordovician–Early Devonian metasedimentary and metavolcanic rocks (Fig. 1). The Meguma Group consists of the metasandstone-dominated Goldenville Formation and overlying slate-dominated Halifax Formation. This series was deformed into NE–SW to N–S trending folds with axial planar cleavage. The majority of shortening is attributed to the Mid-Devonian Acadian Orogeny at ca. 400–385 Ma, based on whole rock and mineral $^{40}Ar/^{39}Ar$ ages (e.g. Keppie and Dallmeyer, 1987; Muecke et al., 1988; Hicks et al., 1999). Regional metamorphism ranges from lower greenschist to amphibolite grade. Voluminous, Middle- to Late-Devonian granitic and lesser mafic plutons (ca. 370 Ma; Harper, 1988; Clarke et al., 1993) truncate regional fold patterns and cleavage. Continued regional northwest-directed transpression of the Meguma Terrane until Permian time is indicated by: dextral displacement on the Cobequid–Chedabucto Fault System (Mawer and

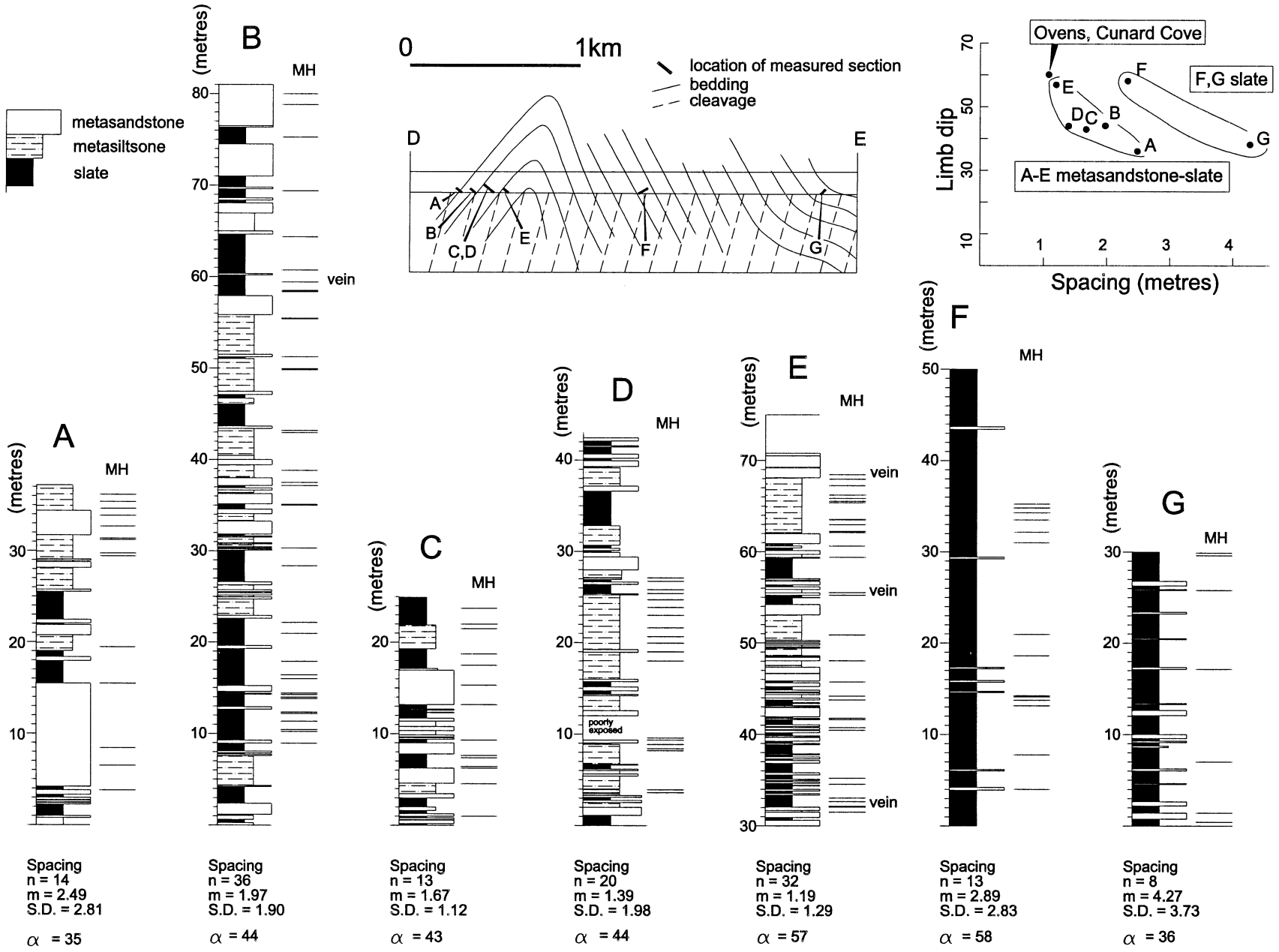
metasandstone
metasiltsone
slate
0
1km
location of measured section
bedding
cleavage
D
E
A
B
C,D
E
F
G
Ovens, Cunard Cove
F,G slate
A-E metasandstone-slate
Limb dip
Spacing (metres)
(metres)
MH
vein
poorly exposed
A
B
C
D
E
F
G
Spacing
n = 14
m = 2.49
S.D. = 2.81
α = 35
Spacing
n = 36
m = 1.97
S.D. = 1.90
α = 44
Spacing
n = 13
m = 1.67
S.D. = 1.12
α = 43
Spacing
n = 20
m = 1.39
S.D. = 1.98
α = 44
Spacing
n = 32
m = 1.19
S.D. = 1.29
α = 57
Spacing
n = 13
m = 2.89
S.D. = 2.83
α = 58
Spacing
n = 8
m = 4.27
S.D. = 3.73
α = 36

White, 1987; Gibbons et al., 1996); syntectonic strain within the South Mountain Batholith (Horne et al., 1992; Benn et al., 1997); Carboniferous shortening of Meguma Group rocks (Culshaw and Liesa, 1997); tectono-thermal events recorded by $^{40}Ar/^{39}Ar$ dating (Kontak and Cormier, 1991; Keppie and Dallmeyer, 1995; Culshaw and Reynolds, 1997); and shortening of Carboniferous rocks (e.g. Boehner, 1991).

Cross-sections of the Meguma Terrane (Fig. 1) show tight- to open- chevron and box style, northwest- and southeast-verging regional folds. Regional cleavage is well-developed, including a fine continuous cleavage in slates and variably developed spaced cleavage in metasandstone. Henderson et al. (1986) proposed that cleavage developed prior to folding and was rotated by simple shear (flexural flow) on the limbs during folding. They suggested that cleavage refraction resulted from differential shear between slate and metasandstone, and that no flexural slip occurred. However, evidence of flexural slip was documented, at least locally, within the Meguma Group by several workers, including Faribault (1899, 1913), Douglas (1948), Keppie (1976), Smith (1976) and O'Brien (1983).

The Meguma Group is host to numerous lode gold occurrences (Fig. 1) and the timing and origin of auriferous quartz veins has prompted considerable debate. Graves and Zentilli (1982), Henderson et al. (1986, 1992) and Henderson and Henderson (1986) proposed that bedding-parallel veins formed prior to regional folding. A variety of syn-folding models were proposed for the bedding-parallel veins by Faribault (1899, 1913), Douglas (1948), Mawer (1987), Keppie (1976) and Williams and Hy (1990). Faribault (1899, 1913) and Douglas (1948) proposed a direct relationship between bedding-parallel veins and flexural slip, and a saddle reef (flexural slip) model was proposed by Keppie (1976). Kontak et al. (1990a) suggested a relationship between auriferous veins and late regional shear zones localized on steep fold limbs.

3. Lawrencetown Anticline

3.1. Setting

We studied the Lawrencetown Anticline in nearly continuous outcrop along the railway tracks in the city of Halifax. This exposure transects the hinge of the anticline within the study area (Fig. 2a and b). The Lawrencetown Anticline in the area is a close (interlimb angle of 65–70°), steeply inclined (73°NW), slightly plunging (10°SW) chevron fold (Figs. 2b and 3). The exposed fold is within the Halifax Formation, which, in the area, consists of interbedded slate, metasiltstone and metasandstone. The hinge zone has a high proportion of thick metasandstone beds (logs A–E, Fig. 3) whereas stratigraphically higher sections consist predominantly of black, sulphide-rich slate and thin (<10 cm) interbedded metasandstone (logs F and G, Fig. 3). The study area is within the aureole of the South Mountain Batholith (Fig. 2), which is responsible for partial annealing of cleavage in slate and locally abundant cordierite porphyroblasts. Quartz veins locally occur within joints and along bedding-parallel surfaces.

3.2. Flexural-slip structures

Both profile and strike-parallel sections are exposed along the railway tracks, allowing for three-dimensional documentation of flexural-slip structures. All movement horizons in the Lawrencetown Anticline were identified by the presence of variably preserved slickenlines and slickenfibers (Figs. 4 and 5b). Numerous bedding-parallel fractures lacking such lineations were discounted, although some may represent movement horizons.

Bedding-parallel movement horizons are almost entirely restricted to slate or metasiltstone lithologies, often at or near lithologic boundaries (Fig. 3). The majority of movement horizons have no marginal deformation, although a domino structure was observed in the footwall of one bedding-parallel movement horizon (Fig. 5d). In profile section, bedding-parallel movement horizons are continuous over the extent of the exposure (several meters). Extensive strike-parallel exposures at the east end of the area reveal along-strike continuity of a few hundred meters for many prominent movement horizons (Figs. 4b and 5a). Others are discontinuous and either die out or link to lateral ramps. The average spacing of the bedding-parallel movement horizons for the measured intervals range from 1.19 to 4.27 m (Fig. 3). Movement horizon spacing decreases with increasing limb dip and slate-dominated sections (logs F and G, Fig. 3) have a notably higher average spacing than the lithologically variable sections for comparable limb dips (graph, Fig. 3).

Structures interpreted to be frontal ramps associated with bedding-parallel movement horizons are parallel to cleavage (compare poles to cleavage (Fig. 2b) with poles to frontal ramps (Fig. 4a)). Where determined, these structures invariably have a reverse sense of movement. There are a few examples of frontal ramps that can be directly traced into bedding-parallel movement horizons as part of flexural-slip duplexes (cf. Tanner, 1992) (Fig. 4b). Structures interpreted to be lateral ramps consist of northwest-trending, northeast-dipping movement horizons (Fig. 4a) coated with quartz slickenfibers. Their intersection with

Fig. 3. Detailed stratigraphic logs of measured sections indicating the location of bedding-parallel movement horizons. Spacing data of movement horizons (MH) are given below each log; n = number of movement horizons, m = the mean spacing, S.D. = the standard deviation, α = limb dip. Location of cross-sections D and E indicated on Fig. 2b. Location of measured sections indicated on cross section and Fig 2b. Inset graph shows the relationship of movement horizon spacing and limb dip for sections from metasandstone-slate (A–E) and slate-dominated (F and G) intervals.

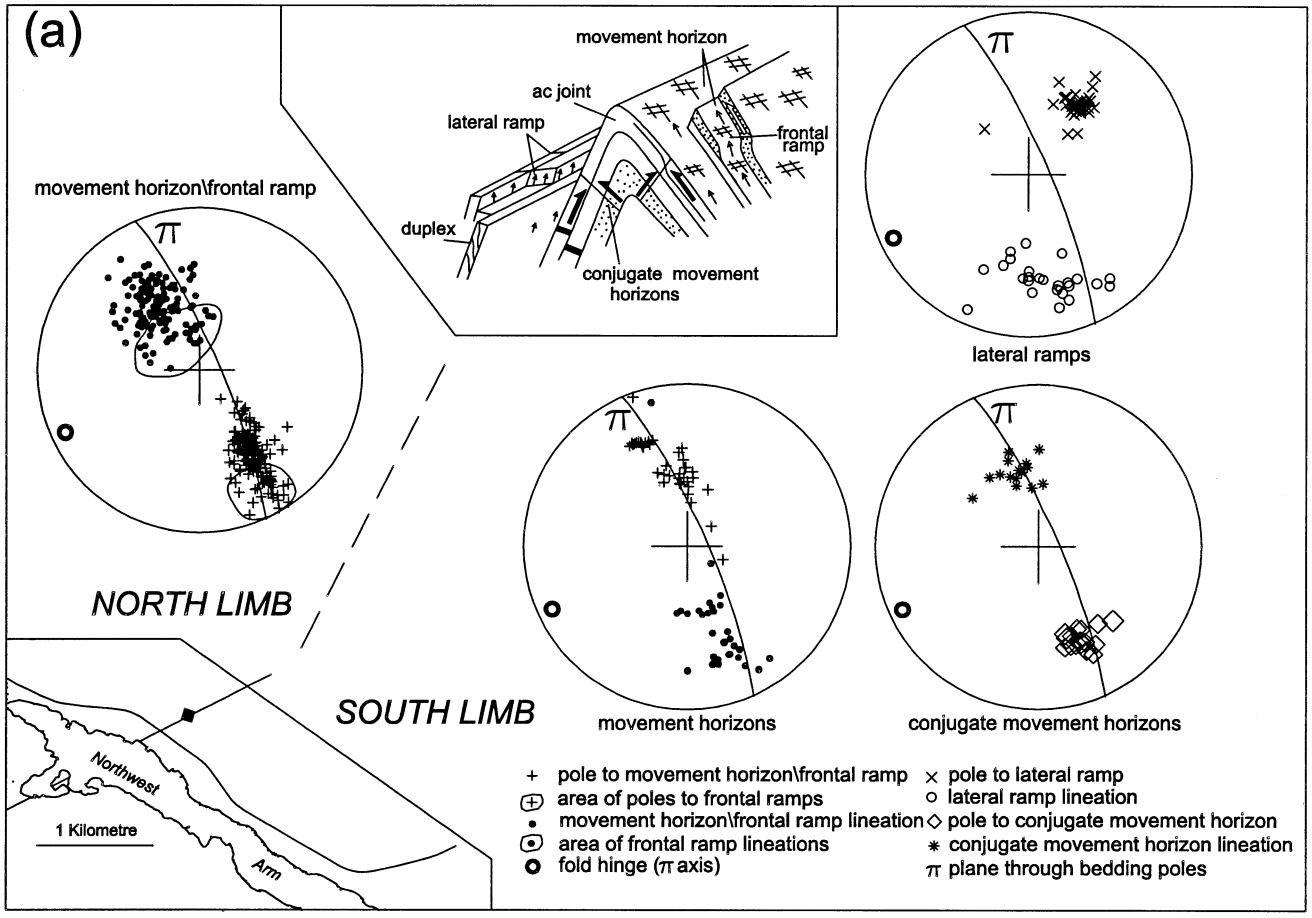

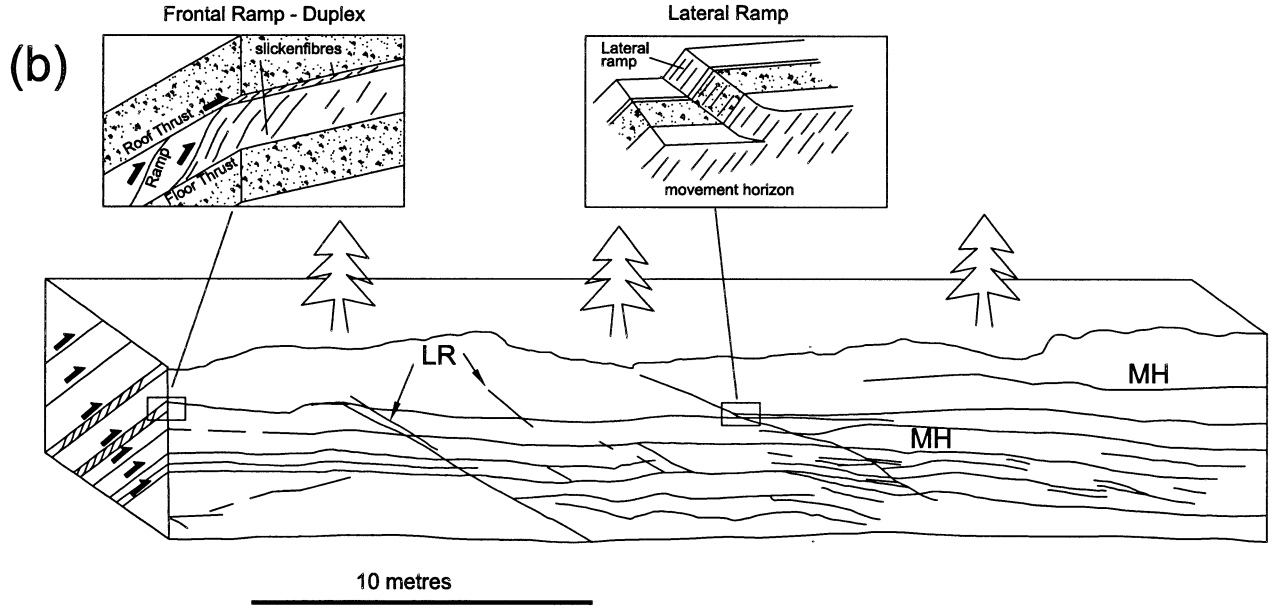

Fig. 4. (a) Equal area stereonets of structural data for the north and south limbs of the Lawrencetown Anticline. Inset illustrates the relationship of flexural-slip structures to the fold. (b) Sketch, from photographs, of a strike-parallel section (location indicated on Fig. 2b), showing the distribution, continuity and relationship of bedding-parallel movement horizons and lateral ramps. Insets illustrate the relationship of lateral and frontal ramps to bedding-parallel movement horizon. MH = bedding-parallel movement horizon, LR = lateral ramp.

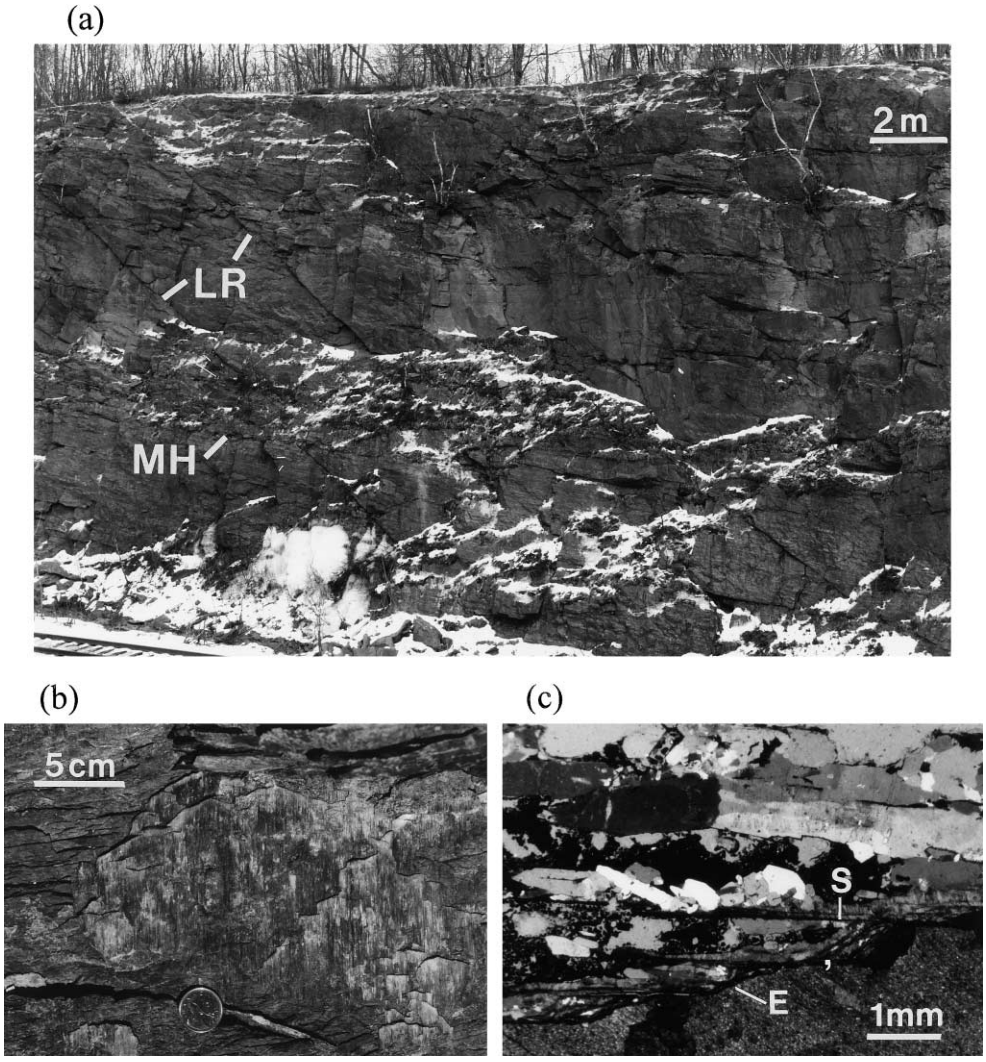

Fig. 5. (a) Photograph of vertical exposure along a strike parallel section, looking to the south, at the east end of the railway tracks (portion of Fig. 4b) showing bedding-parallel movement horizons (MH) and lateral ramps (LR). Note railway tracks in lower left for scale. (b) Photograph of slickenfiber-coated bedding-parallel movement horizon from the railway section. (c) Photomicrograph of slickenfiber cut perpendicular to the movement horizon and parallel to slickenfiber lineation. Note step geometry of wall rock margin defined by extensional (E) and shear (S) sectors (cf. Ramsay and Huber, 1983). Shear sense is top to the left. (d) Photograph of flexural-slip domino structure in footwall of bedding-parallel movement horizon showing top to the left sense of movement. EV = extensional veins. (e) Sketch illustrating the original conjugate relation of bedding-parallel movement horizons (MH) and shears bounding dominoes. δ = the acute angle between bedding-parallel movement horizons and shears bounding dominoes. (f) Sketch illustrating the finite relation of the domino structure to the fold resulting from flexural-slip shear. EV and δ as above; ω = the angle of rotation of dominoes. EV and shear sense of dominoes are consistent with flexural slip. (g) Photomicrograph of slickenfiber and wallrock cut perpendicular to movement horizon and parallel to slickenfiber. Note abundant cordierite (cd), many with muscovite pressure shadows (ps) developed parallel to cleavage (S_1). (h) Sketch illustrating how pressure shadows in (g) are consistent with fold-related strain.

bedding-parallel movement horizons is parallel to movement direction lineations on both structures and the sense of shear is the same. Some lateral ramps can be observed to link with bedding-parallel movement horizons. (Fig. 4b). Lateral ramps vary from outcrop-scale (Figs. 4b and 5a), which are through going structures, to centimeter-scale, which typically link closely-spaced bedding-parallel movement horizons. Locally, highly discordant movement horizons with a shear sense antithetic to the bedding-parallel movement horizons (conjugate movement horizons, inset Fig. 4a) are also part of the linked system.

3.3. Movement direction and shear sense

Shear sense on flexural-slip movement surfaces was determined by slickenfiber geometry (Fig. 5b and c), frontal ramp and flexural-slip duplex geometry (Fig. 4b) and domino structures (Fig. 5d), and invariably shows a reverse shear sense which changes across the fold. Slickenfiber-wall rock boundaries are characterized by a stepped geometry (Fig. 5c) representing extensional and shear fractures formed during movement horizon development (Ramsay and Huber, 1983; Fowler, 1996). The domino structures are bounded by bedding-parallel movement horizons, with

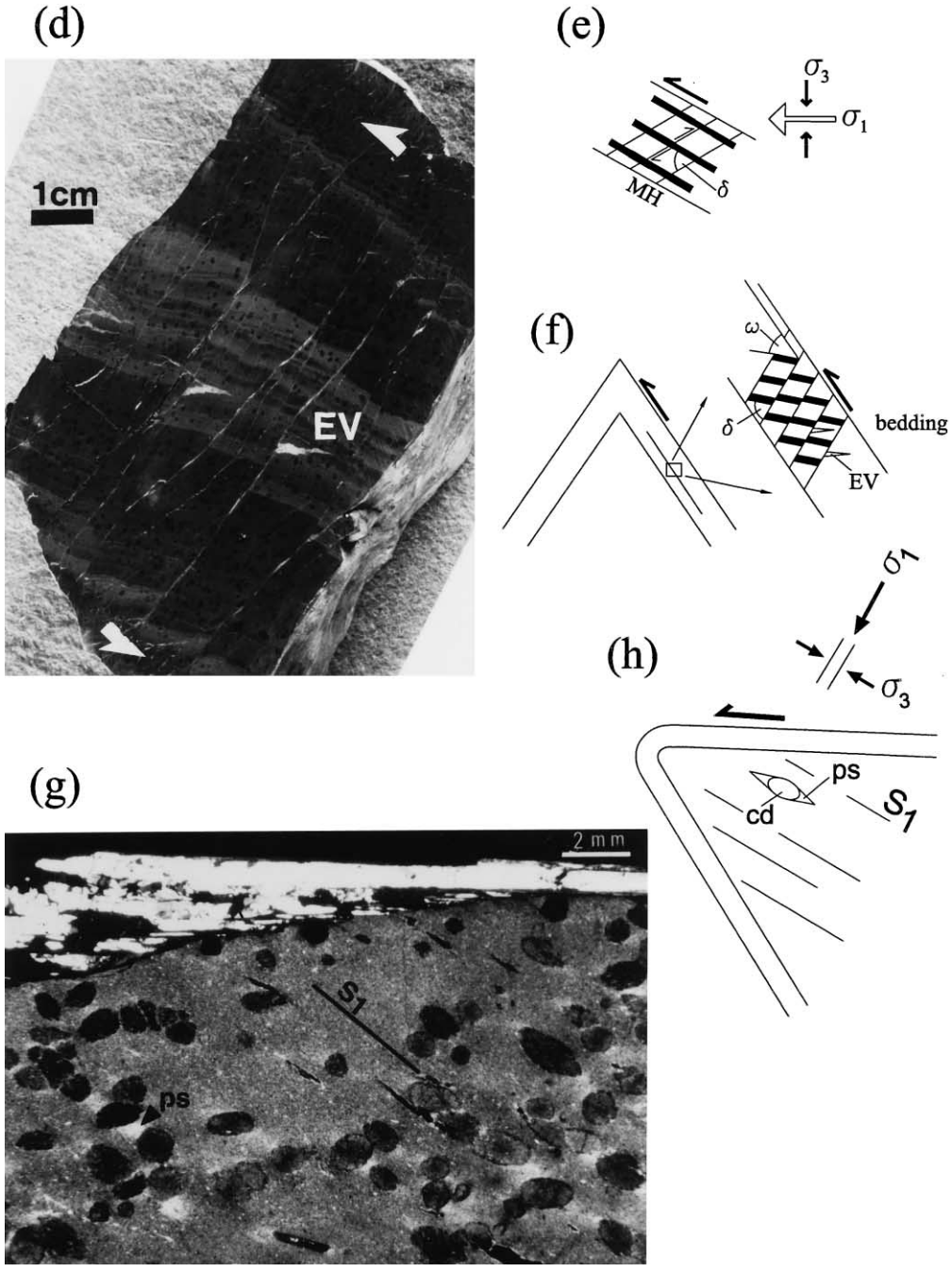

Fig. 5. (*continued*)

slickensided shear fractures between the rotated blocks. The initial angle between the shear fractures and the bedding-parallel movement horizons can be inferred from the angle between the bedding laminations and shear fractures (δ, Fig. 5e and f). The inferred angle and the opposing shear sense on the two surfaces is consistent with an initial conjugate relationship between them (Fig. 5e).

On average, movement lineations on bedding-parallel movement horizons, frontal ramps and lateral ramps do not plunge perpendicular to the gently inclined anticlinal hinge (i.e. they do not fall on the π plane), but rather the average trend is down the dip of bedding on both limbs (Fig. 4a). This suggests flexural slip reflects fold growth after plunge development.

3.4. Timing of flexural slip

Cordierite porphyroblasts formed in the contact aureole of the ca. 370 Ma South Mountain Batholith are locally truncated by flexural-slip structures indicating at least some flexural slip occurred after or late in the history of granite intrusion. The occurrence of strain shadows around cordierite, which define a lineation within the cleavage

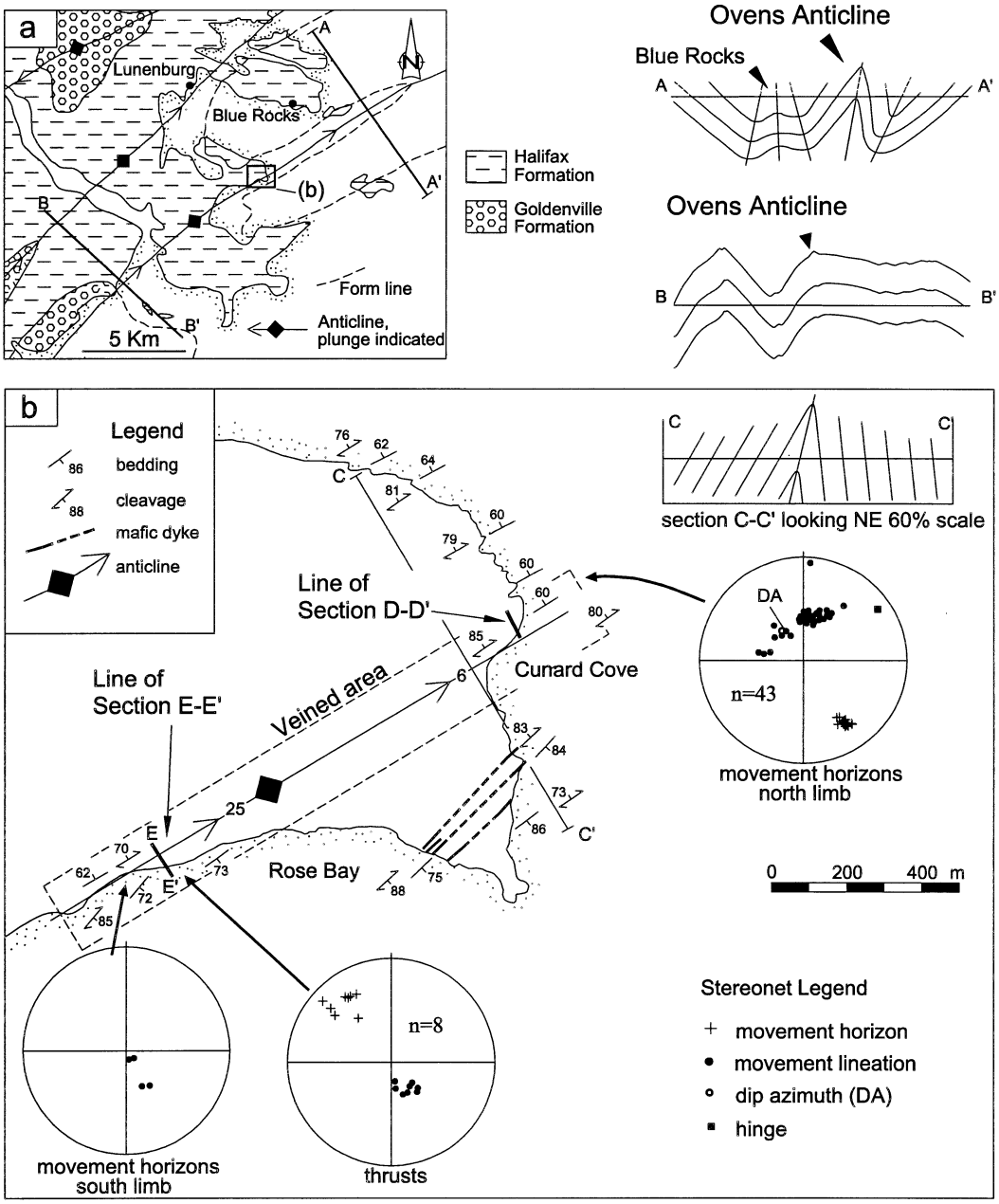

Fig. 6. (a) Simplified geological map and cross-section of the Lunenburg area showing the location of the Ovens study area (map and section A–A′ modified after O'Brien, 1988; section B–B′ modified after Faribault (1929)). (b) Geological map and cross-section of the Ovens area showing the location of the Cunard Cove and Rose Bay areas and sections. Stereonets of flexural-slip movement horizons and lineations for the north (Cunard Cove) and south (Rose Bay) limb of the Ovens Anticline and thrusts from Zone B (Fig. 7b) in Rose Bay.

plane and which are generally consistent with flexural flow (Fig. 5g and h), indicate some ductile, fold-related strain between movement horizons that postdates granite emplacement and which may be coeval with flexural slip.

4. Ovens study area

4.1. Setting

The Ovens Anticline is located along the Atlantic coast south of Lunenburg (Figs. 1 and 6). The anticline occurs within the lower Halifax Formation and stratigraphy is similar to that exposed in the Lawrencetown Anticline; interbedded slate and metasandstone in the hinge zone and predominantly slate at higher stratigraphic levels. The closest major exposed intrusion is the South Mountain Batholith, outcropping ~25 km to the north (Fig. 1), although minor dykes occur within the area (Fig. 6b). Regional folds adjacent to the Ovens Anticline include chevrons and modified box folds; variation in fold profile along the hinge (Fig. 6a) reflects noncylindrical fold geometry.

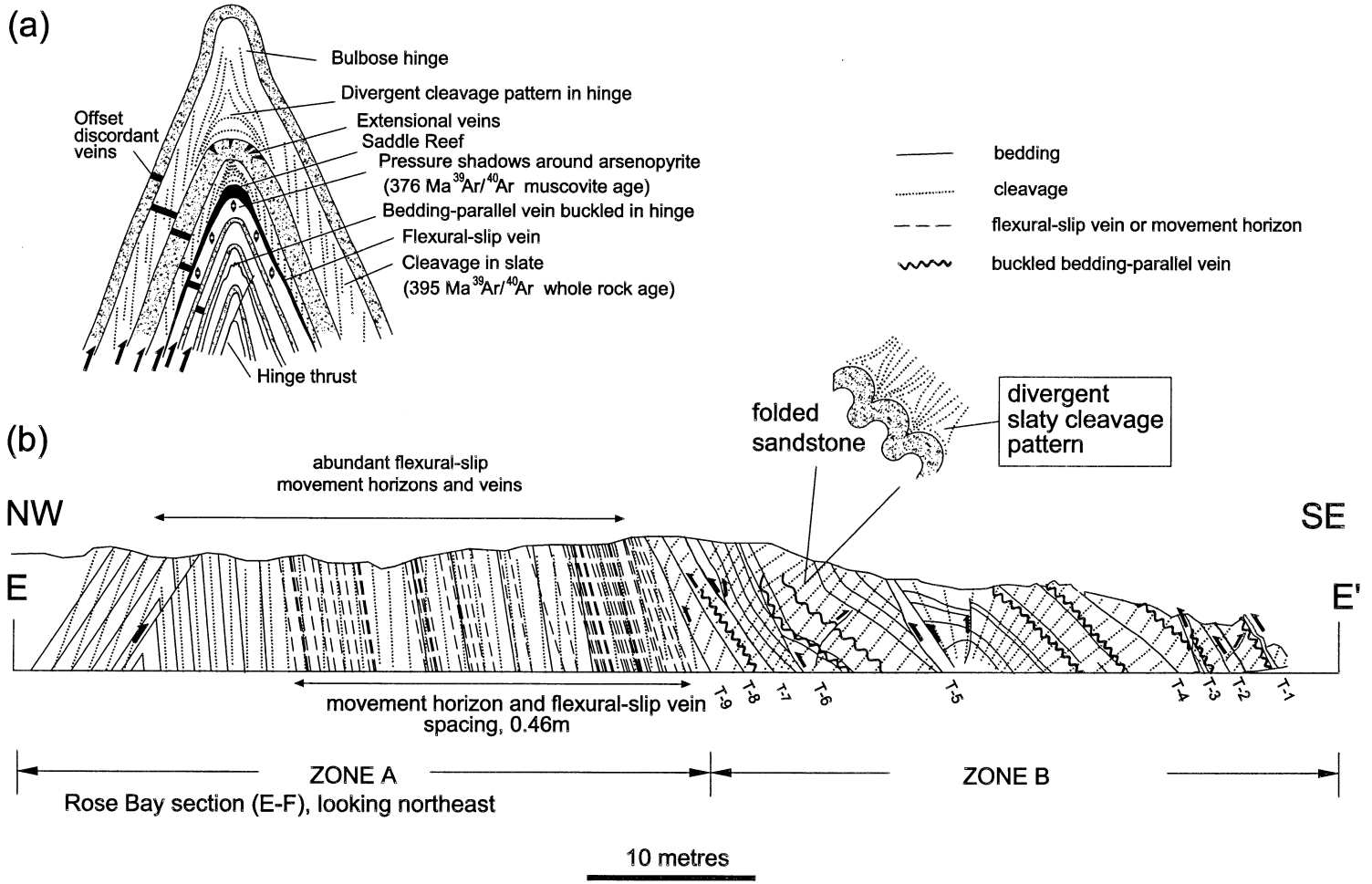

Fig. 7. (a) Schematic cross-section of the Ovens Anticline illustrating structural features in the hinge area. (b) Cross-section of the hinge area and south limb of the Ovens Anticline in Rose Bay area (drawn from photographs) illustrating the contrast in the structural character of the hinge region (Zone A) and a thrusted section of the south limb (Zone B); see text for discussion.

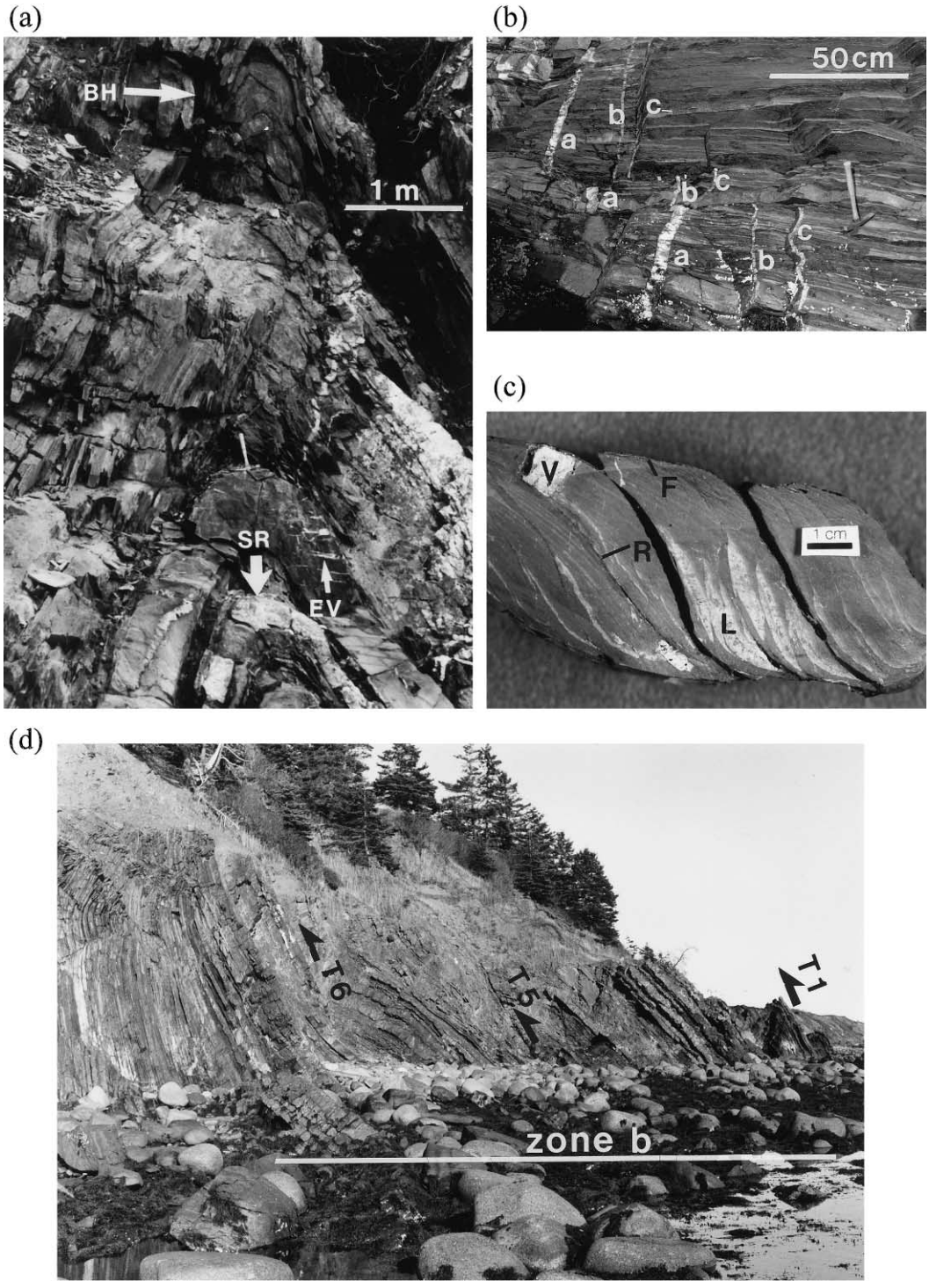

Fig. 8. (a) Photograph of the hinge of the Ovens Anticline exposed in Rose Bay showing the narrow hinge zone and straight limbs, a saddle reef vein (SR), extensional veins (EV) in the outer arc of a metasandstone bed and a bulbous hinge form (BH); hammer in fold crest above saddle reef for scale. (b) Photograph showing strike separation of discordant veins displaced by flexural slip. Note variation in spacing of veins (lettered a, b and c) along different flexural-slip movement horizons, reflecting dip-slip offset of variably dipping, conjugate veins (see Fig. 11); hammer is 29 cm long. (c) Photograph of a cut slab of a flexural-slip duplex showing ramp (R) and flat (F) geometry and imbrication of sedimentary layering (L) and a discordant quartz vein (V); slab cut parallel to movement lineations and perpendicular to movement horizon. (d) Photograph of part of the south limb of the Ovens Anticline in the Rose Bay area showing the thrust sheets in Zone B (profile view looking to the northeast). Thrusts T-1, T-5 and T-6 indicated; compare with Fig. 7b.

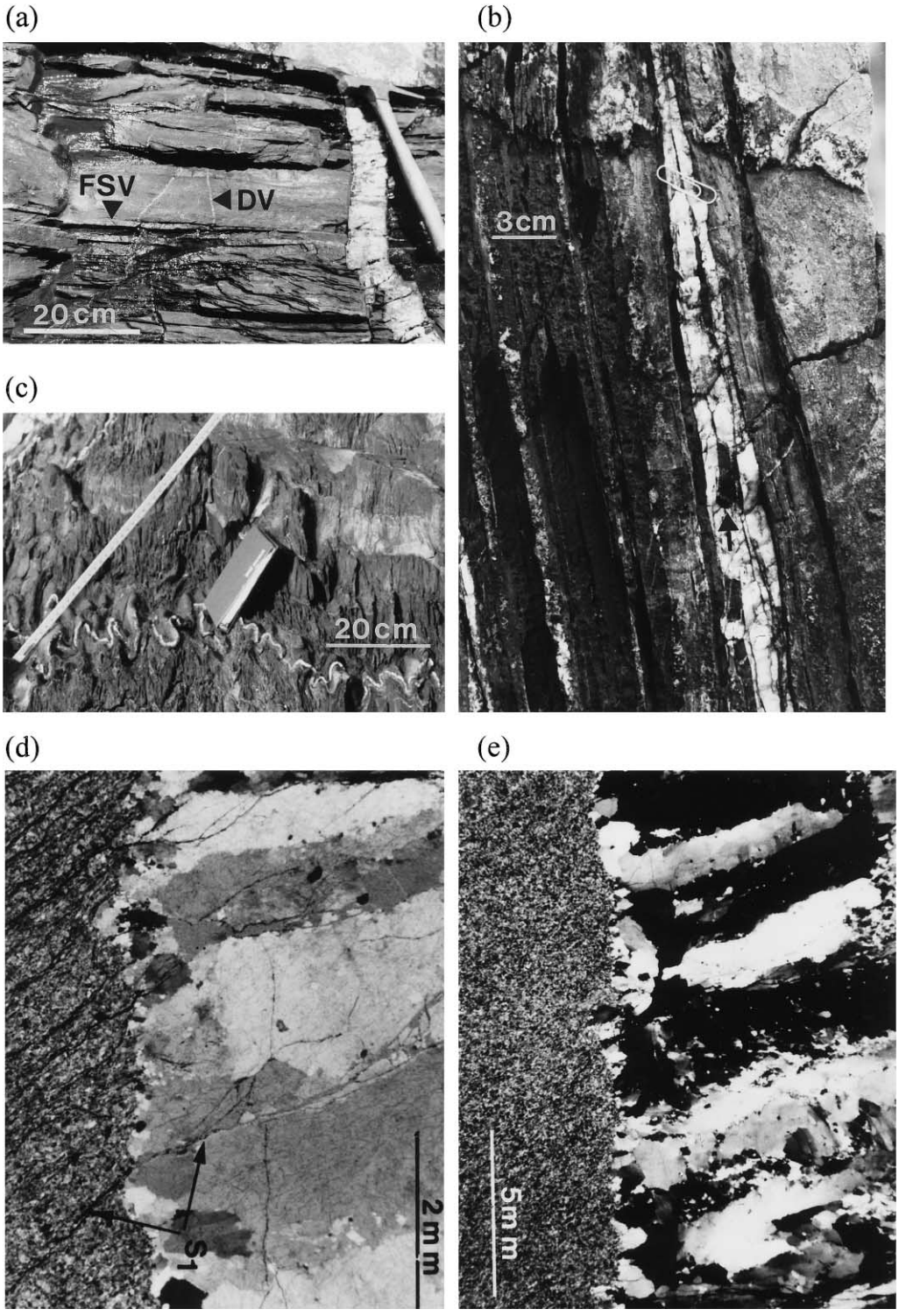

Fig. 9. (a) Photograph of flexural-slip bedding-parallel veins (FSV) along movement horizons defined by offset discordant veins (DV). The discordant vein at right is not offset and therefore postdates flexural slip, suggesting synchronous emplacement of flexural-slip and discordant veins. (b) Photograph of typical flexural-slip vein showing laminated nature, pinch and swell character and inclusions of cleaved slate fragments (arrow); profile view. (c) Photograph of buckled bedding-parallel vein in the hinge of the Ovens Anticline. (d) Photomicrograph of discordant vein (plane polarized light) showing continuation of cleavage (S_1) from host metasandstone into vein. (e) Photomicrograph of discordant vein (under crossed polars) showing fibrous quartz displaying undulose extinction and local subgraining.

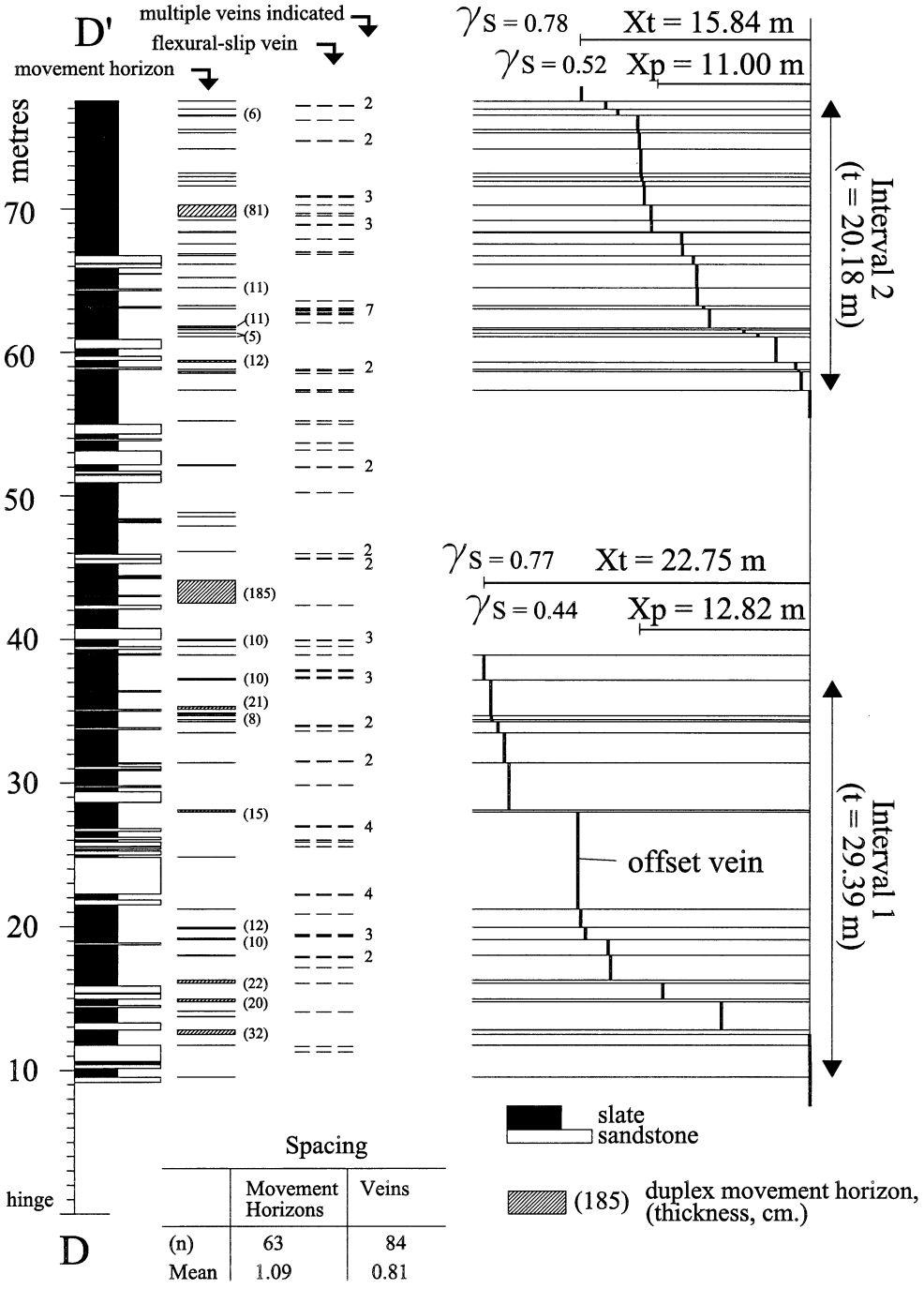

Fig. 10. Stratigraphic-structural log of section D–D′, north limb of the Ovens Anticline; bottom of section located at the hinge exposed in Cunard Cove (location of section indicated on Fig. 6b). Bedding-parallel movement horizons and flexural-slip bedding-parallel veins are indicated to the right of stratigraphic log and spacing data are given at the bottom of log; n = number of movement horizons. Slip amount calculated for movement horizons from offset veins for two intervals of the log is illustrated graphically to the right. The cumulative slip amounts for each interval are given as the total cumulative offset (X_T) and the corrected offset (X_P), the latter representing the slip amount projected in the profile plane of the fold. Flexural-slip shear strain (γ_S) given to the left of cumulative offsets. Method of determining slip amount is shown in Fig. 11.

In the study area, the Ovens Anticline is a tight (interlimb angle of 35–40°) steeply inclined (~77°NW), gently plunging (6–25°NE) chevron fold (Fig. 6b). Structural features in the hinge area are typical of chevron folds, including local accommodation structures such as hinge thrusts, bulbous hinges and saddle reefs (Figs. 7a and 8a). Metasandstone beds, in which tangential longitudinal strain has locally produced extensional veins in the outer arc (Ramsay, 1967), maintain thickness across the hinge, whereas slate beds are thicker in the hinge (Figs. 7a and 8a). Fine continuous cleavage within slate is axial planar on the limbs. However, close to the outer arc of metasandstone

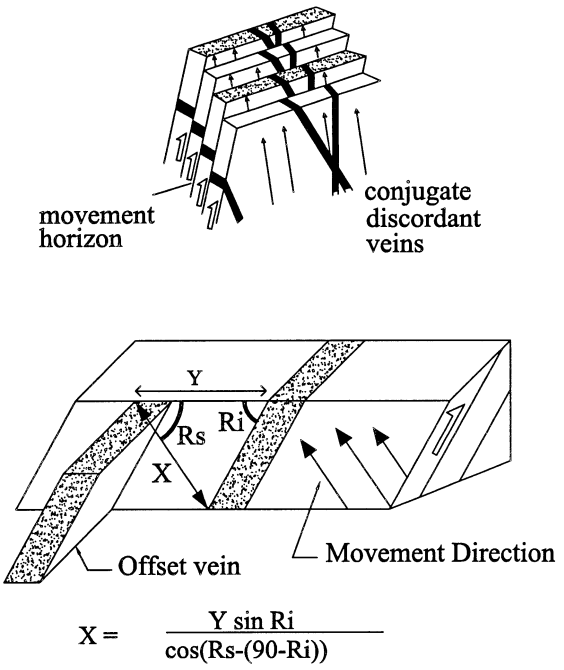

Fig. 11. Schematic diagram showing the relation of offset, conjugate discordant veins to flexural-slip movement horizons at the Ovens, and schematic diagram showing the method used to determine the slip amount, X; where Y = strike separation, R_i = rake of the intersection of the offset vein on the movement horizon and R_s = rake of the movement direction on the movement horizon.

hinges the cleavage has a divergent triangular pattern surrounding a neutral point (Fig. 7a) resulting from inverse tangential longitudinal strain (Ramsay and Huber, 1987) in the slate adjacent to metasandstone beds. A poorly developed spaced cleavage in the metasandstone lies at a high angle to bedding throughout the fold. Quartz–muscovite pressure shadows adjacent to arsenopyrite define a down-dip stretching lineation within the cleavage plane in the hinge area (Fig. 7a).

Both fold limbs are planar, with no minor parasitic folds, and there are abundant bedding-parallel movement horizons related to flexural slip. On the south limb there are several outcrop-scale thrusts separating blocks in which cleavage dips at a high angle to the axial plane of the anticline (Zone B, Fig. 7b).

Whole rock (slate) $^{40}Ar/^{39}Ar$ ages of ca. 395–399 Ma from the hinge area of the Ovens Anticline (Fig. 7a) and the thrust sheets (Fig. 7b) record the main phase of Acadian deformation and metamorphism (Kontak et al., 1998). In contrast, an $^{40}Ar/^{39}Ar$ age of ca. 376 Ma for muscovite in pressure shadows around arsenopyrite from the hinge area (Fig. 7a) has been interpreted to reflect late, fold-related strain (Hicks et al., 1999).

4.2. Flexural slip

Detailed investigation of flexural slip was carried out on the north limb in Cunard Cove (Section D–D′, Fig. 6a), and on the south limb adjacent the hinge in Rose Bay (Zone A, Section E–E′, Fig. 7b). The principal flexural-slip structures in the Ovens area are bedding-parallel movement horizons and were identified by offset of quartz veins that are discordant to bedding (henceforth 'discordant veins') (Figs. 7a, 8b and 9a). Movement horizons include thin, polished slip planes with striations and slickenfibers (quartz, calcite and sulphide), and flexural-slip duplexes (Tanner, 1992). Thin slip planes have no marginal deformation and their presence is often evident only by displacement of the discordant veins. Quartz veins are common along movement horizons (Figs. 7a and 9a and b). These veins commonly have striated margins and are interpreted to have been emplaced during flexural-slip (henceforth 'flexural-slip veins'); flexural-slip veins are described more fully below.

Flexural-slip duplexes consist of sigmoidal, rotated slate horses with polished and striated cleavage-parallel slip planes bounded by bedding-parallel movement horizons. Sedimentary layering is imbricated across the cleavage-parallel slip planes (Fig. 8c). Breccia zones are developed along the floor or roof thrusts of some duplex zones and, in some instances, brecciation has deformed (flexural-slip) quartz veins along these movement horizons. Flexural-slip duplexes range in thickness from <2 to 185 cm and most flexural-slip duplexes have uniform thickness when observed in profile sections.

4.3. Movement direction-sense of shear

Movement lineations from the south limb (Zone A, Rose Bay) trend approximately perpendicular to the hinge (Fig. 6b). Movement lineations from the north limb in Cunard Cove show considerable variation in trend, from perpendicular to highly oblique to the fold hinge (Fig. 6b) and two lineations were noted on some movement horizons, indicating variation in slip direction through time. These features may reflect lateral hinge propagation during non-cylindrical, flexural-slip fold growth, where slip in the fold terminations in the early stages of folding, which is oblique to the hinge, is overprinted by slip perpendicular to the hinge after hinge propagation (Dubey, 1982).

Shear sense was determined from displaced conjugate veins (Fig. 7a), slickenfiber geometry and flexural-slip duplex geometry (Fig. 8c). It is invariably a reverse sense of shear that systematically changes across the fold hinge.

4.4. Continuity and spacing of movement horizons

The excellent exposure in Cunard Cove and Rose Bay allows the observation that movement horizons are continuous at the same stratigraphic level for the ~10–20 m of profile exposure in both areas and for up to 200 m of strike-parallel exposure in Rose Bay. The location of movement horizons in a measured section in Cunard Cove (Section D–D′) are shown in Fig. 10. All movement horizons occur within slate layers, frequently near slate-metasandstone boundaries. The average spacing of

Table 1
Table of slip amount data for flexural-slip movement horizons in two intervals of Section D–D′, Cunard Cove (see Fig. 10). Location refers to the stratigraphic position measured from the hinge, X_T is the slip amount along the movement horizon, X_P is the slip amount projected into the fold profile plane, spacing is the distance to movement horizon above and duplex refers to flexural-slip duplexes, indicated by D. All measurements are in meters

Interval 1					Interval 2				
Location	X_T	X_P	Spacing	Duplex	Location	X_T	X_P	Spacing	Duplex
38.91	0.07	0.05	0.59		77.52	1.65	0.7		
37.16	0.48	0.34	1.75	D	76.96	0.85	0.41	0.56	
34.67	0.04	0.03	2.49		77.48	1.38	0.69	0.48	D
34.39	0.05	0.04	0.28		75.54	0.03	0.02	0.94	
34.26	0.41	0.3	0.13		75.33	0.08	0.05	0.21	
33.49	0.44	0.36	0.77		73.19	0.11	0.07	1.14	
31.4	0.31	0.23	2.09		72.49	0.01	0.01	0.7	
27.95	4.79	1.75	3.45	D	72.23	0.07	0.06	0.26	
24.82	0.01	0.01	3.13		71.94	0.12	0.09	0.29	
21.21	0.2	0.14	3.61		71.60	0.04	0.02	0.34	
19.95	0.33	0.32	1.26	D	69.47	0.47	0.24	2.13	D
19.1	1.57	1.28	0.85	D	69.21	0.03	0.02	0.26	
18.02	0.16	0.14	1.08		68.43	0.35	0.22	0.78	
16.05	3.62	2.56	1.97	D	68.37	1.74	1.43	0.06	
14.75	4.05	1.71	1.3	D	67.56	0.06	0.04	0.81	
13.72	0.03	0.02	1.03		66.73	0.75	0.75	0.83	
12.48	6.11	3.51	1.24	D	66.15	0.24	0.24	0.58	
11.73	0.02	0.02	0.75		64.42	0.04	0.02	1.73	D
9.52	0.03	0.03	2.21		63.26	0.44	0.28	1.16	
					63.04	0.41	0.25	0.22	
					61.7	2.04	1.59	1.34	D
					61.58	0.35	0.27	0.12	
					61.34	0.96	0.84	0.24	D
					61.09	1.27	0.93	0.25	
					59.31	1.36	0.96	1.78	D
					58.81	0.21	0.21	0.5	
					58.66	0.18	0.14	0.15	
					57.34	0.6	0.45	1.32	
Total	12.82	22.75			Total	15.84	11		

movement horizons for Section D–D′ is 1.09 m, and flexural-slip duplexes are intermixed with simple slip planes (Fig. 10).

We note that numerous bedding-parallel veins that are similar in character to flexural-slip veins occur along horizons where no slip is indicated by displaced discordant veins (Fig. 10). These veins may reflect flexural-slip movement horizons active prior to emplacement of discordant veins.

Including these bedding-parallel veins as movement horizons gives an average spacing of 0.52 m for Section D–D′ (Fig. 10) and a similar spacing of movement horizons plus bedding-parallel veins (0.46 m) was determined in Zone A of Section E–E′ (Fig. 7b).

4.5. Flexural-slip displacement, shear strain and change of limb dip

Offset of discordant quartz veins across flexural-slip movement horizons allows for direct determination of the amount of slip that has occurred since vein emplacement (Fig. 11). Slip amount along flexural-slip movement horizons was determined for two intervals of Section D–D′ in Cunard Cove, where movement lineations were observed and offset veins could be matched across movement horizons. The slip amount along movement horizons in the two intervals are given in Table 1 and shown graphically in Fig. 10. The cumulative slip for each interval is given as the uncorrected cumulative total slip parallel to variably trending displacement vectors (X_T). A corrected value, the cumulative profile slip amount (X_P), represents the slip amount for each movement horizon projected onto the fold profile plane. Flexural-slip shear strain (γ_S) represented by offset veins (slip amount/interval thickness) for the two intervals of Section D–D′ are similar (Fig. 10), suggesting that these values are representative of the fold limb in general. The average value of γ_S for the two intervals is 0.78 for the uncorrected slip amount (X_T) and 0.48 for the corrected profile plane slip amount (X_P).

For angular upright chevron folds generated primarily by flexural folding, the total shear strain is equivalent to the tangent of limb dip and may include components of flexural flow and flexural slip (Ramsay, 1974; Tanner, 1989). The amount of limb dip change due to a given increment of flexural-slip shear strain depends critically on the limb dip at which that increment is applied. In the Ovens Anticline,

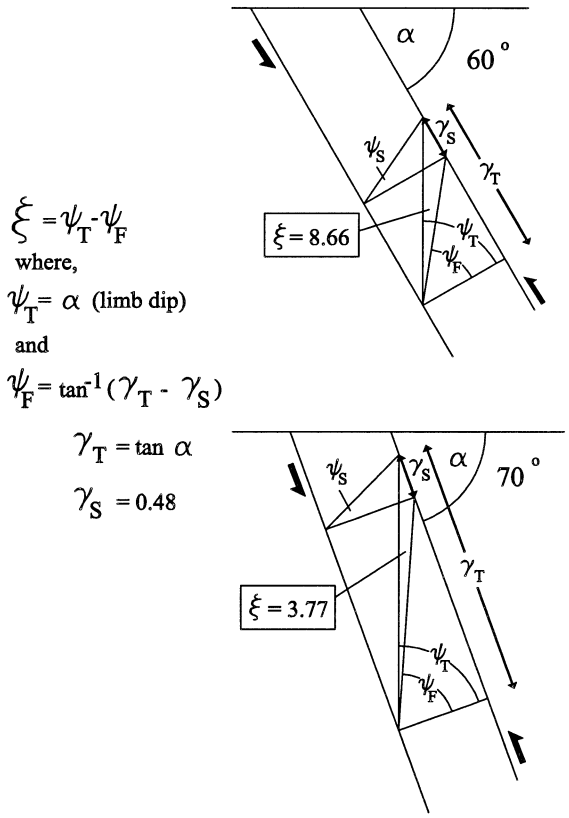

Fig. 12. Diagram showing the method of determining the change in limb dip (ξ) resulting from flexural-slip shear strain, assuming flexural slip accounts for the last increment of folding and flexural flow accounts for earlier folding. The change in limb dip depends on the limb dip at the beginning of flexural slip, and, for a constant increment of flexural-slip shear strain the change of limb dip decreases with increasing initial limb dip. ψ_T = the total angular shear strain from flexural folding, ψ_F = angular flexural flow strain, γ_T = total shear strain, γ_S = flexural-slip shear strain (value given, 0.48, is the average corrected flexural-slip shear strain for intervals 1 and 2 of section D–D′; Fig. 10). Values of ξ determined for final limb dips of 60° and 70°.

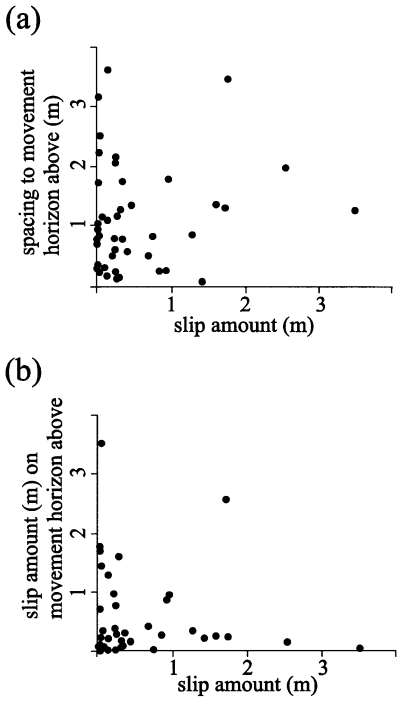

Fig. 13. Plots of (a) slip amount on flexural-slip movement horizons against spacing to the movement horizon stratigraphically above and (b) slip amount on flexural-slip movement horizons against slip amount on the movement horizon stratigraphically above for intervals 1 and 2 of section D–D′. Slip amounts given are the corrected values (X_P, Table 1). No correlation is evident in either plot.

flexural slip represents a very late increment of folding: flexural-slip duplexes deform cleavage, cleaved slate fragments occur in flexural-slip veins (see below), flexural-slip veins and synchronous discordant veins show minimal evidence of deformation (see below), and movement horizons show no evidence of later deformation. Fig. 12 shows the change in limb dip (ξ) resulting from the measured flexural-slip shear strain (0.48; i.e. γ_S for corrected slip), assuming that flexural slip represents the last increment of folding. This value has been determined for final limb dips of 60° and 70°, values that correspond to, respectively, the measured limb dip and the limb dip relative to the axial plane (i.e. 90° − 1/2 interlimb angle) for the north limb in Cunard Cove. For a 60° final limb dip, the measured flexural-slip shear strain accounts for the last approximately 9° of limb dip, and for a 70° final limb dip the flexural-slip shear strain accounts for approximately 4° of limb dip. We note that inclusion of all bedding-parallel veins similar in character to those along movement horizons as slip surfaces would clearly increase the contribution of flexural slip to folding and thus increase the change in limb dip due to flexural slip.

4.6. Relationship between slip amount and movement horizon spacing

Theoretical and experimental studies of flexural slip typically assume contemporaneous formation of movement horizons, with simultaneous slip on all movement horizons (e.g. Ramsay, 1974; Behzadi and Dubey, 1980). However, some studies suggest that increasing shear during progressive flexural-slip folding is accommodated by formation of new movement horizons as well as further movement on existing ones. This was the explanation given for an observed decrease of movement horizon spacing with increasing limb dip (Tanner, 1989) and for an observed non-linear relationship between slip amount (inferred from vein thickness) and movement horizon spacing (Fowler and Winsor, 1997).

Plots of slip amount against distance to the closest movement horizon stratigraphically above (Fig. 13a) or slip amount on the movement horizon stratigraphically above (Fig. 13b) for the two intervals of Section D–D′ in Cunard Cove are similar to data presented by Fowler and Winsor (1997), with no correlation between these parameters. As discussed by Fowler and Winsor (1997), a lack of

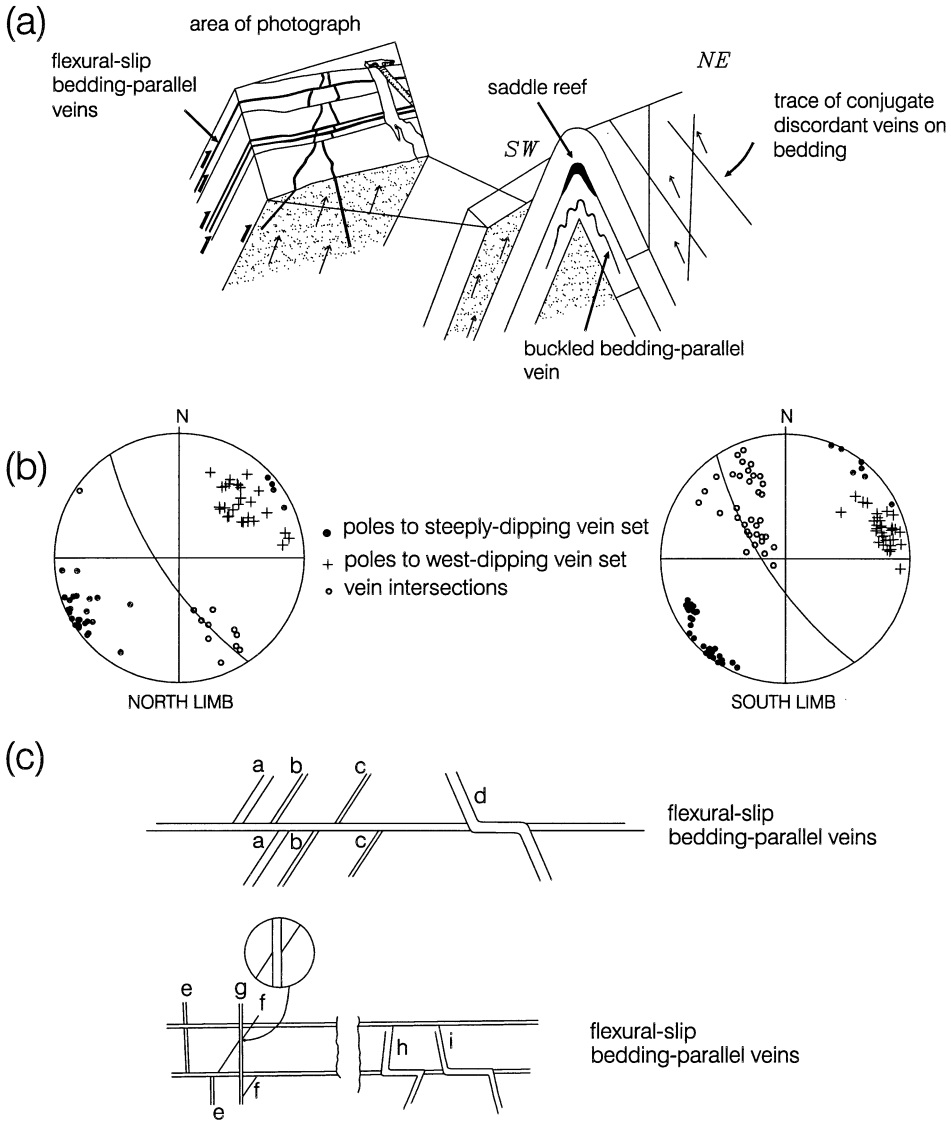

Fig. 14. (a) Schematic diagram showing the relationship of vein sets to the fold geometry for the Ovens Anticline. Block diagram of flexural-slip veins to the left drawn from Fig. 9a. (b) Stereonets of poles to conjugate discordant vein pairs (steep and west-dipping), and their intersections, for the north and south limbs of the Ovens Anticline. (c) Schematic diagrams (plan view) showing two examples of the relationship between flexural-slip veins and conjugate discordant veins. Discordant veins a, b, c and e are offset across flexural-slip veins, indicating they predate the flexural-slip veins, whereas discordant veins f and g cut flexural-slip veins indicating they postdate the flexural-slip vein. Discordant veins d, h and i show apparent offset along flexural-slip veins, however they are continuous along, and cut, the flexural-slip vein. This suggests offset of a discordant fracture, with vein emplacement after, or during, flexural slip. These mutual cross-cutting relations imply synchronous emplacement of flexural-slip and discordant veins during flexural-slip folding.

correlation between slip and movement horizon spacing is inconsistent with simultaneous slip on all movement horizons resulting from folding, and suggests that the slip-spacing data reflects progressive initiation of new movement horizons with variable spacing. A model of flexural slip involving progressive formation of new movement horizons is supported in the Ovens Anticline by mutual cross-cutting relationships between flexural-slip movement horizons (veins) and discordant veins (see quartz veins below) and in the Lawrencetown Anticline by decreasing movement horizon spacing with increasing limb dip.

4.7. Thrusts

Several outcrop-scale thrust sheets and associated structures occur on the south limb in Rose Bay (Zone B, Figs. 7b and 8d). Thrust surface features (e.g. striations, laminated veins, duplexes) are similar to those on flexural-slip movement horizons. Reverse displacement, perpendicular to the fold hinge (Fig. 6b), is indicated by offset stratigraphy, bedding-parallel veins (e.g. T-3, Fig. 7b) and discordant veins and the geometry of slickenfibers, duplexes and the thrust system.

The internal structure of the thrust sheets is characterized

by large bedding-cleavage angles and symmetric minor folds, contrasting markedly with adjacent fold limbs (Fig. 7b). The angle between bedding and cleavage is constant throughout fault-related folds (Fig 7b), indicating cleavage development before thrusting. Bedding-cleavage angles and symmetric minor fold geometry in the thrust sheets suggests that they originated in the hinge area of a fold and were emplaced onto the anticline limb without significant internal modification.

4.8. Quartz veins

Abundant quartz veins occur in the hinge area of the Ovens Anticline (veined area Fig. 6b). Veins include both bedding-parallel and discordant veins and the large majority of veins are related to the flexural-slip event. Bedding-parallel veins include buckled veins, flexural-slip veins and saddle reefs (Fig. 14a). Flexural-slip veins are defined by their occurrence along movement horizons (Figs. 7a, 9a, 10 and 14a), however, as noted previously, there are similar bedding-parallel veins where flexural slip is not evident by displacement of discordant veins. Flexural-slip veins are planar, commonly display a pinch and swell geometry and are locally laminated (contain vein-parallel wall rock inclusion layers; Baker, 1996) (Fig. 9b) or vuggy. Some veins contain angular, rotated fragments of cleaved wall rock (Fig. 9b), demonstrating post-cleavage formation, although in thin section flexural-slip veins exhibit ductile strain (undulose extinction, subgrains). Some flexural-slip veins are down-dip extensions of saddle reef veins. Tightly buckled bedding-parallel veins are restricted to hinge zones, occurring in the narrow hinge zone of the Ovens Anticline (Figs. 9c and 14a) and within the thrust sheets on the south limb (Fig. 7b). Graves (1976), Graves and Zentilli (1982) and Henderson et al. (1986, 1992) proposed that these buckled bedding-parallel veins represent parasitic folds, which record layer-parallel shortening prior to regional folding. However, restriction of buckled veins to hinge zones supports a synfolding origin for these minor folds, where layer-parallel shortening in the hinge zone accompanied flexural shear on the limbs (c.f. Williams and Hy, 1990). Also, as noted above, angular chevron and box folds like those of the Meguma Group initiate and amplify with little layer-parallel shortening (Ramsay and Huber, 1987). These observations support a common, synfolding origin for bedding-parallel veins (i.e. buckled bedding-parallel, flexural-slip and saddle reef veins) in the Ovens area. However, we note that some buckled veins may predate the flexural-slip event.

Discordant conjugate veins occur throughout the hinge area of the Ovens Anticline and are in many places displaced across movement horizons (Figs. 7a, 8b, 9a and 14a) and thrust surfaces. Intersecting veins were classified as steeply-dipping and west-dipping and their orientations are consistent throughout the area (Fig. 14b). Vein geometry is clearly related to that of the fold: the obtuse bisector of paired conjugate veins is sub-parallel to the fold hinge and their intersection (calculated) lies dispersed within the ac plane (Fig. 14b). Although most discordant veins are planar, some exhibit minor buckling and all veins are cut by a spaced cleavage which is continuous with cleavage in the host (Fig. 9d). In thin section discordant veins exhibit undulose extinction, subgrains and recrystallized grains (Fig. 9e).

Mutual cross-cutting relationships exist between flexural-slip and discordant veins (Fig. 9a and 14c), indicating synchronous emplacement of both vein sets during flexural-slip folding. A common origin for these veins explains why both bedding-parallel and discordant veins are concentrated in the hinge zone and have similar accessory minerals (gold, scheelite and sulphide minerals).

5. Discussion

Our study has shown that flexural slip in the folds studied was late, relative to flexural flow, and although it was accompanied by abundant quartz veins and some spectacular minor structures it accounts for relatively little fold growth. We discuss below the results of our findings with respect to the timing of flexural slip, the flexural-slip mechanism, the association of thrusting and flexural-slip folding and the potential significance of flexural slip in the formation of gold deposits in the Meguma Group.

5.1. Timing of flexural slip

Flexural slip is a brittle deformation that occurred late in fold development, whereas the early phase of folding (Henderson et al., 1986) took place under regional metamorphic conditions. Flexural slip was not only late in the folding history, accounting for the last increments of limb dip in chevron folds, but there is also evidence that it was a Late Devonian (ca. 370 Ma) event and thus separated from the Acadian (ca. 385–400 Ma) flexural flow stage by a considerable interval. For example, flexural-slip structures in the Lawrencetown Anticline deform cordierite reflecting contact metamorphism by the ca. 370 Ma South Mountain Batholith. An $^{40}Ar/^{39}Ar$ age of ca. 376 Ma for muscovite in pressure shadows in the hinge of the Ovens Anticline (Hicks et al., 1999) contrasts significantly with whole rock $^{40}Ar/^{39}Ar$ ages of ca. 400 Ma from the same locality (Kontak et al., 1998) (Fig. 7a) and 388–395 Ma from the Meguma Group in the surrounding area (Hicks et al., 1999), which are interpreted to reflect cleavage development. The younger age suggests the pressure shadows reflect fold-related strain which postdates the main phase of cleavage development and which may be coincident with the flexural-slip event. Brittle flexural slip structures have been documented throughout the Meguma Group (see introduction), suggesting a regional significance for the late flexural-slip documented in the folds studied. This is supported by a ca. 370 Ma age for quartz vein emplacement at several Meguma gold deposits ($^{40}Ar/^{39}Ar$; Kontak et al., 1990b),

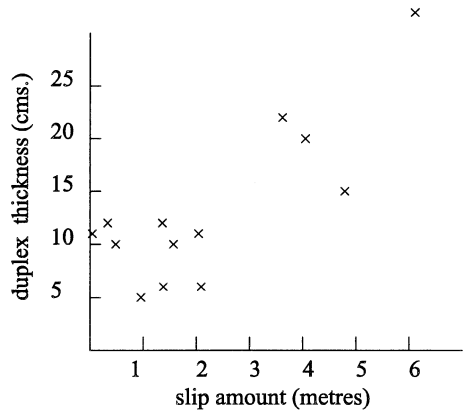

Fig. 15. Graph of the thickness of flexural-slip duplexes against the amount of slip measured along the duplex (X_T, Table 1).

which we suggest have a flexural-slip origin (see below). The ca. 370 Ma flexural-slip event is unlikely to have been continuous with the early flexural-flow phase of folding that took place under regional metamorphic conditions between 15 and 30 m.y. earlier. Reactivation of the fold belt is consistent with evidence for post-Acadian regional transpression of the Meguma Terrane, in particular, syntectonic strain recorded within the Late Devonian South Mountain Batholith (Benn et al., 1997). Transition from ductile flexural flow to brittle flexural slip may reflect unroofing and cooling of the orogen in the intervening 15–30 m.y.

5.2. Flexural-slip mechanism

Many of the flexural-slip structures identified in this study are well known and comparable with those documented by Tanner (1989, 1992) (bedding-parallel movement horizons, flexural-slip duplexes, flexural-slip veins, slickenfibers). However, we have also documented additional structures not previously observed related to flexural slip. These include the interconnected bedding-parallel, lateral ramp, frontal ramp and conjugate movement horizons in the Lawrencetown Anticline (inset Fig. 4a). The existence of the linked system of movement horizons shows how flexural-slip structures may develop in three dimensions in a fashion comparable with ramp and flat thrust belts.

The magnitude of shear strain recorded by displacement of the discordant quartz veins in the Ovens Anticline is a significant portion of the total fold-related shear strain. However, because flexural slip occurs when the limbs of the chevron fold are already steeply dipping, it accounts for only a small change in limb dip (Fig. 12). Bedding-parallel veins not included as movement horizons may represent unaccounted flexural slip, and thus the contribution of flexural slip to folding may be underestimated. Including these veins as movement horizons would approximately double their number and thus, assuming a similar average slip amount for these movement horizons as for those measured, the total flexural-slip shear strain would be approximately twice that measured.

As discussed above, Tanner (1989) and Fowler and Winsor (1997) proposed a flexural-slip model with progressive formation of new movement horizons during folding. However, these studies lacked constraints on the timing of flexural slip and slip amount. Tanner (1989) speculated that flexural flow may be important in the early stages of folding, with flexural slip becoming more important late in the folding history. Fowler and Winsor (1997) present a computer model of flexural-slip activity that produces a relationship between spacing and slip amount similar to that between spacing and vein thickness data for natural folds. In the model, flexural-slip activity extends from limb dips of 10° to 70°. Our data show a similar relationship between spacing and slip amount as that presented by Fowler and Winsor (1997), even though flexural slip accounts for only the last approximately 10° of limb dip. If the actual slip amounts in the natural fold described by Fowler and Winsor (1997) is significantly less than that required for folding, then flexural slip activity in those folds may also be restricted to the final stages of folding. Indeed, Fowler (1996) notes that flexural-slip bedding-parallel veins in these folds formed during or after cleavage related to folding. Restriction of flexural slip to the later stages of folding could reflect the increasing rate of shear strain with increasing limb dip (for a constant rate of shortening) or, as suggested above, moving from ductile to brittle conditions as a result of uplift.

The variable nature of flexural-slip structures may be a reflection of the progressive development of new movement horizons. For example, the mixture of discontinuous and continuous movement horizons in the Lawrencetown Anticline (Fig. 4b) likely reflects an assortment of early-(continuous) movement horizons, along which significant slip has occurred, and late-formed (discontinuous) movement horizons where slip is minor. Frontal and lateral ramps may be another way of increasing the area of movement horizons available for slip. In the Ovens Anticline flexural-slip duplexes record more slip than simple movement horizons (Table 1) and there is a positive correlation between the amount of slip and duplex thickness (Fig. 15). This suggests that flexural-slip duplexes develop from simple movement horizons only after considerable displacement has occurred and represent the oldest movement horizons.

The common occurrence of slickenfibers and veins along flexural-slip structures (Tanner, 1989; Fowler and Winsor, 1997; this study) indicate the presence of a fluid during flexural slip. Cosgrove (1993) suggested a 'stick-slip' history for flexural-slip folding resulting from fluctuating fluid pressure, where episodes of slip are restricted to periods of high fluid pressure when the normal stress on movement horizons is reduced. Given the steep limb dips for the Ovens Anticline, and thus high normal stress on bedding, high fluid pressure would almost seem a prerequisite for flexural slip. Fluctuating and high fluid pressure is

supported by fluid inclusion data from flexural-slip veins in the Ovens Anticline (Baker, 1996). Some fluid inclusion data indicate pressures which may be supralithostatic; pressures inferred from fluid inclusions are higher than those inferred from metamorphic assemblages (Baker, 1996). Fold-related ductile strain broadly coeval with flexural slip, including pressure shadows on cordierite in the Lawrencetown Anticline and arsenopyrite in the Ovens Anticline and minor buckling and microstructural evidence for ductile deformation recorded in the flexural-slip vein array in the Ovens Anticline, may reflect deformation between episodes of flexural slip.

5.3. Thrusting and fold development

The minor structures in the thrust sheets resemble those in the flat hinge segment of a box fold, such as the syncline in the Blue Rocks area (Fig. 6a). The internal structure of the thrust sheets indicates that thrusting postdates cleavage formation and several features suggest that thrusting was coeval with the brittle flexural-slip event. Thrust surfaces are similar to flexural-slip movement horizons and thrusting is kinematically consistent with flexural slip. Thrusts are cut by, and offset, discordant veins interpreted to be emplaced during flexural slip. The presence of veins along thrusts suggest that, like flexural slip, thrusting was assisted by fluid pressure. We suggest, therefore, a common timing and origin for flexural slip and thrusting at the Ovens, with flexural slip on limbs of chevrons and the emplacement of thrust sheets, originating in the flat tops of box folds, recording the same episode of shortening under brittle conditions.

In the Lachlan Fold Belt of Australia, where there is a comparable mix of box and chevron fold geometries as the Meguma Group, Fowler and Winsor (1996) suggested, on the basis of comparison of natural folds and analog experiments, that chevron folds developed progressively from box folds. We suggest this is also the case for the Meguma folds, basing our claim on the along-strike variation in the fold profile of the Ovens Anticline, which changes along its hinge from a box fold (B–B′, Fig. 6a) to a chevron in the vicinity of the study area (A–A′, Fig. 6a). The thrusting recorded at the Ovens may reflect a mechanism of box fold to chevron transition under brittle conditions. Along strike variation from box folds to chevrons requires lateral propagation during the box fold to chevron transition, which could explain the oblique trend of movement lineations on the north limb of the Ovens Anticline (Fig. 6b). Similar examples of thrusting and flexural slip may be expected elsewhere in the Meguma Group or in other box-chevron fold environments. We emphasize that, regionally, both the box-to-chevron transition and lateral hinge propagation need not have been restricted to the period of flexural slip, but could have accompanied earlier flexural-flow folding.

5.4. Meguma gold deposits

As stated in the introduction, the origin of Meguma gold deposits has been attributed to various pre- to syn-folding models. Our study demonstrates a primarily flexural-slip origin for the vein array at the Ovens Anticline. Of particular significance regarding the origin of Meguma gold deposits is the restriction of buckled veins to fold hinges, which we interpret to reflect layer-parallel shortening during folding in contrast to layer-parallel shortening prior to folding (e.g. Graves, 1976; Henderson et al., 1986). The vein array at the Ovens shows similarity to vein arrays described throughout the Meguma Terrane; vein arrays generally occur in the hinges of anticlines, veins are concentrated on steep limbs (where flexural-slip strain is high) and bedding-parallel veins generally occur in slate intervals (where movement horizons occur) (e.g. Faribault, 1899, 1913; Malcom, 1929; Graves and Zentilli, 1982; Henderson and Henderson, 1986; Sangster, 1990). Therefore, we suggest a flexural-slip model is a reasonable general model that explains the character of the vein arrays for most Meguma gold deposits.

Acknowledgements

RJH extends thanks to Steve Haysom for his assistance and patience in measuring sections and to Colin MacDonald, Darcy Baker and Lisa MacDonald for field assistance. We are grateful to Dave Cameron, operator of the Ovens Natural Park, for allowing access to the Ovens Park and his support of the project. The comments of T. Wright, M.J. Markley, J.D. Crider and an anonymous reviewer improved this manuscript. D. Kontak, P. Smith and R. Jamieson and, especially, J.W. Waldron provided helpful discussions. This paper is published with the permission of the Director of Minerals and Energy Division, Nova Scotia Department of Natural Resources. The work was also supported by an NSERC operating grant to NC.

References

Baker, D.E.L., 1996. Fluid inclusions and microstructure of flexural-slip bedding-concordant veins within the Ovens Anticline, Lunenburg, Nova Scotia. Unpublished B.Sc. thesis, Dalhousie University, Halifax, Nova Scotia.

Behzadi, H., Dubey, A.K., 1980. Variation of interlayer slip in space and time during flexural folding. Journal of Structural Geology 2, 453–457.

Benn, K., Horne, R.J., Kontak, D.J., Pignotta, G., Evans, N.G., 1997. Syntectonic emplacement of the South Mountain Batholith, Meguma Terrane, Nova Scotia: magnetic fabric and structural analysis. Geological Society of America Bulletin 109, 1279–1293.

Biot, M.A., 1965. Mechanics of Incremental Deformation. Wiley, New York, 505pp.

Boehner, R.C., 1991. Seismic interpretation: potential overthrust geology and mineral deposits in the Kennetcook Basin, Nova Scotia. In: MacDonald, D.R. (Ed.). Mines and Mineral Branch, Report of Activities 1990. Nova Scotia Department of Mines and Energy Report 91-1, pp. 37–47.

Chapple, W.M., Spang, J.H., 1974. Significance of layer-parallel slip during folding of layered sedimentary rocks. Geological Society of America Bulletin 85, 1523–1534.

Clarke, D.B., MacDonald, M.A., Reynolds, P.H., Longstaffe, F.J., 1993. Leucogranites from the eastern part of the South Mountain Batholith. Journal of Petrology 34, 653–679.

Cobbold, P.R., Cosgrove, J.W., Summers, J.M., 1971. Development of internal structures in deformed anisotropic rocks. Tectonophysics 12, 23–53.

Cosgrove, J.W., 1993. The interplay between fluids, folds and thrusts during deformation of a sedimentary succession. Journal of Structural Geology 15, 491–500.

Culshaw, N., Liesa, M., 1997. Alleghanian reactivation of the Acadian fold belt, Meguma Zone, southwest Nova Scotia. Canadian Journal of Earth Sciences 34, 833–847.

Culshaw, N., Reynolds, P., 1997. $^{40}Ar/^{39}Ar$ age of shear zones in the southwest Meguma Zone between Yarmouth and Meteghan, Nova Scotia. Canadian Journal of Earth Sciences 34, 848–853.

Douglas, G.V., 1948. Structure of the gold veins of Nova Scotia. In: Structural Geology of Canadian Ore Deposits 1, Canadian Institute of Mining and Metallurgy Jubilee Volume, pp. 919–926.

Dubey, A.K., 1982. Development of interlayer slip in non-cylindrical flexural slip folds. Geoscience Journal 3 (2), 103–108.

Dubey, A.K., Cobbold, P.R., 1977. Noncylindrical flexural slip folding in nature and experiment. Tectonophysics 38, 223–239.

Faribault, E.R., 1899. On the gold measures of Nova Scotia and deep mining. The Canadian Mining Review 18 (3), 78–82.

Faribault, E.R., 1908. City of Halifax. Canada Department of Mines, Geological Survey Branch, Map 68, scale 1:63,360.

Faribault, E.R., 1913. The gold deposits of Nova Scotia. The Canadian Mining Journal 34 (22), 108–109 also 24, 780–781.

Faribault, E.R., 1929. Bridgewater. Canada Department of Mines, Geological Survey Branch, Map 89, scale 1:63,360.

Fletcher, H., Faribault, E.R., 1911. Southeast Nova Scotia. Canada Department of Mines, Geological Survey, Map 53A, scale 1:250,000.

Fowler, T.J., 1996. Flexural slip generated bedding-parallel veins from central Victoria, Australia. Journal of Structural Geology 18, 1399–1415.

Fowler, T.J., Winsor, C.N., 1996. Evolution of chevron folds by profile shape changes: comparison between multilayer deformation experiments and folds of the Bendigo-Castlemaine goldfields, Australia. Tectonophysics 258, 125–150.

Fowler, T.J., Winsor, C.N., 1997. Characteristics and occurrence of bedding-parallel slip surfaces and laminated veins in chevron folds the Bendigo–Castlemaine goldfields: implications for flexural-slip folding. Journal of Structural Geology 19, 799–815.

Gibbons, W., Doig, R., Gordon, T., Murphy, B., Reynolds, P., White, J.C., 1996. Mylonite to megabreccia: Tracking fault events within a transcurrent terrane boundary in Nova Scotia, Canada. Geology 24, 411–414.

Graves, M.C., 1976. The formation of gold-bearing quartz veins in Nova Scotia: Hydraulic fracturing under conditions of greenschist regional metamorphism during early stages of deformation. Unpublished M.Sc. thesis, Dalhousie University, Halifax, Nova Scotia, Canada.

Graves, M.C., Zentilli, M., 1982. A review of the geology of gold in Nova Scotia. In: Hodder, R.W., Petruk, K.W. (Eds.). Geology of Canadian Gold Deposits. Canadian Institute of Mining and Metallurgy, Special Volume 24, pp. 233–242.

Harper, C.L., 1988. On the nature of time in the cosmological perspective. Unpublished Ph.D. thesis, Oxford University.

Henderson, M.N., Henderson, J.R., 1986. Constraints on the origin of gold in the Meguma Zone, Ecum Secum area, Nova Scotia. Maritime Sediments and Atlantic Geology 22, 1–13.

Henderson, J.R., Wright, T.O., Henderson, M.N., 1986. A history of cleavage and folding: and example from the Goldenville Formation, Nova Scotia. Geological Society of America Bulletin 97, 1354–1366.

Henderson, J., Wright, T., Henderson, M., 1992. Strain history of the Meguma Group, Lunenburg and Ecum Secum areas, Nova Scotia. Geological Association of Canada, Mineralogical Association of Canada Joint Annual Meeting, Wolfville, Nova Scotia; Field Excursion C-11: Guidebook.

Hicks, R.J., Jamieson, R.A., Reynolds, P.H., 1999. Detrital and metamorphic $^{40}Ar/^{39}Ar$ ages from muscovite and whole rock samples, Meguma Supergroup, southern Nova Scotia. Canadian Journal of Earth Sciences 36, 23–32.

Horne, R.J., MacDonald, M.A., Corey, M., Ham, L., 1992. Structure and emplacement of the South Mountain Batholith. Atlantic Geology 28, 29–50.

Hudleston, P.J., Treagus, S., Lan, L., 1996. Flexural flow folding: Does it occur in nature?. Geology 24, 203–206.

Keppie, J.D., 1976. Structural model for the saddle reef and associated gold veins in the Meguma Group, Nova Scotia. Canadian Institute of Mining and Metallurgy Transactions 69, 103–116.

Keppie, J.D., 1979. Geological Map of Nova Scotia. Nova Scotia Department of Mines and Energy, Nova Scotia, scale 1:50,000.

Keppie, J.D., Dallmeyer, R.D., 1987. Polyphase late Paleozoic tectonothermal evolution of the southwestern Meguma Terrane, Nova Scotia: evidence from $^{40}Ar/^{39}Ar$ mineral ages. Canadian Journal of Earth Sciences 24, 1242–1254.

Keppie, J.D., Dallmeyer, R.D., 1995. Late Paleozoic collision, delamination, short-lived magmatism, and rapid denudation in the Meguma Terrane (Nova Scotia, Canada): constraints from $^{40}Ar/^{39}Ar$ isotopic data. Canadian Journal of Earth Sciences 32, 644–659.

Kontak, D.J., Cormier, R.F., 1991. Geochronological evidence for multiple tectono-thermal overprinting events in the East Kemptville muscovite-topaz leucogranite, Yarmouth County, Nova Scotia, Canada. Canadian Journal of Earth Sciences 28, 209–224.

Kontak, D.J., Smith, P.K., Kerrich, R., Williams, P.F., 1990a. Integrated model for Meguma Group lode gold deposits, Nova Scotia, Canada. Geology 18, 238–242.

Kontak, D.J., Smith, P.K., Reynolds, P., Taylor, K., 1990b. Geological and $^{40}Ar/^{39}Ar$ constraints on the timing of quartz vein formation in the Meguma Group lode-gold deposits, Nova Scotia. Atlantic Geology 26, 201–277.

Kontak, D.J., Horne, R.J., Sandeman, H., Archibauld, D., Lee, J.K.W., 1998. $^{40}Ar/^{39}Ar$ dating of ribbon-textured veins and wall rock material from Meguma lode gold deposits, Nova Scotia: Implications for timing and duration of vein formation in slate-belt hosted vein gold deposits. Canadian Journal of Earth Sciences 35, 746–761.

Malcom, W., 1929. Gold Fields of Nova Scotia. Geological Survey of Canada, Memoir, 385.

Markley, M., Wojtal, S., 1996. Mesoscopic structure, strain, and volume loss in folded cover strata, Valley and Ridge Province, Maryland. American Journal of Science 296, 23–57.

Mawer, C.K., 1987. Mechanics of formation of gold-bearing quartz veins, Nova Scotia, Canada. Tectonophysics 135, 99–119.

Mawer, C.K., White, J.C., 1987. Sense of displacement on the Cobequid–Chedabucto fault system, Nova Scotia, Canada. Canadian Journal of Earth Sciences 24, 217–223.

Muecke, G.K., Elias, P., Reynolds, P.H., 1988. Hercynian/Alleghanian overprinting of an Acadian Terrane: $^{40}Ar/^{39}Ar$ studies in the Meguma Zone, Nova Scotia. Chemical Geology 73, 153–167.

O'Brien, B.H., 1983. The structure of the Meguma Group between Gegogan Harbour and Country Harbour, Guysborough County. In: Mills, K.A. (Ed.). Mines and Minerals Branch, Report of Activities, 1992. Nova Scotia Department of Mines and Energy Report 83-1, pp. 145–181.

O'Brien, B.H., 1988. A study of the Meguma Terrane in Lunenburg County, Nova Scotia. Geological Survey of Canada Open File Report 1823.

Price, N.J., Cosgrove, J.W., 1990. Analysis of Geological Structures. Cambridge University Press, Cambridge.

Ramsay, J.G., 1967. Folding and Fracturing of Rocks. McGraw-Hill, New York.

Ramsay, J.G., 1974. Development of chevron folds. Geological Society of America Bulletin 85, 1741–1754.

Ramsay, J.G., Huber, M.I., 1983. The Techniques of Modern Structural Geology, Volume 1: Strain Analysis. Academic Press, London.

Ramsay, J.G., Huber, M.I., 1987. The Techniques of Modern Structural Geology, Volume 2: Folds and Fractures. Academic Press, London.

Sangster, A.L., 1990. Metallogeny of the Meguma Terrane, Nova Scotia. In: Sangster, A.L. (Ed.). Mineral Deposits of Nova Scotia, Vol. 1. Geological Survey of Canada, Paper 90-8, pp. 115–162.

de Sitter, L.U., 1958. Boudins and parasitic folds in relation to cleavage and folding. Geologie en Mijnbouw 20, 277–286.

Smith, P.K., 1976. The structural geology of the south-eastern part of the Kentville area (21H/2E), Nova Scotia. Unpublished M.Sc. thesis, Acadia University, Wolfville, Nova Scotia, Canada.

Tanner, P.W.J., 1989. The flexural slip mechanism. Journal of Structural Geology 11, 635–655.

Tanner, P.W.J., 1992. Morphology and geometry of duplexes formed during flexural slip folding. Journal of Structural Geology 14, 1173–1192.

Williams, P.F., Hy, C., 1990. Origin and deformational and metamorphic history of gold-bearing quartz veins on the Eastern Shore of Nova Scotia. In: Sangster, A.L. (Ed.). Mineral Deposits of Nova Scotia, Vol. 1. Geological Survey of Canada, Paper 90-8, pp. 169–194.